

Constraining Torsion with Gravity Probe B*

Yi Mao,¹ Max Tegmark,^{1,2} Alan H. Guth,¹ and Serkan Cabi¹

¹*Dept. of Physics, Massachusetts Institute of Technology, Cambridge, MA 02139*

²*MIT Kavli Institute for Astrophysics and Space Research, Cambridge, MA 02139*

(Dated: Submitted to Phys. Rev. D. 1/8-07; Revised 9/18-07; Accepted 9/27-07)

It is well-entrenched folklore that all torsion gravity theories predict observationally negligible torsion in the solar system, since torsion (if it exists) couples only to the intrinsic spin of elementary particles, not to rotational angular momentum. We argue that this assumption has a logical loophole which can and should be tested experimentally, and consider non-standard torsion theories in which torsion can be generated by macroscopic rotating objects. In the spirit of action=reaction, if a rotating mass like a planet can generate torsion, then a gyroscope would be expected to feel torsion. An experiment with a gyroscope (without nuclear spin) such as Gravity Probe B (GPB) can test theories where this is the case.

Using symmetry arguments, we show that to lowest order, any torsion field around a uniformly rotating spherical mass is determined by seven dimensionless parameters. These parameters effectively generalize the PPN formalism and provide a concrete framework for further testing GR. We construct a parametrized Lagrangian that includes both standard torsion-free GR and Hayashi-Shirafuji maximal torsion gravity as special cases. We demonstrate that classic solar system tests rule out the latter and constrain two observable parameters. We show that Gravity Probe B is an ideal experiment for further constraining non-standard torsion theories, and work out the most general torsion-induced precession of its gyroscope in terms of our torsion parameters.

PACS numbers: 04.25.Nx, 04.80.Cc

I. INTRODUCTION

Einstein's General Theory of Relativity (GR) has emerged as the hands down most popular candidate for a relativistic theory of gravitation, owing both to its elegant structure and to its impressive agreement with a host of experimental tests since it was first proposed about ninety years ago [1–3]. Yet it remains worthwhile to subject GR to further tests whenever possible, since these can either build further confidence in the theory or uncover new physics. Early efforts in this regard focused on weak-field solar system tests, and efforts to test GR have since been extended to probe stronger gravitational fields involved in binary compact objects, black hole accretion and cosmology [4–35].

A. Generalizing general relativity

The arguably most beautiful aspect of GR is that it geometrizes gravitation, with Minkowski spacetime being deformed by the matter (and energy) inside it. As illustrated in Figure 1, for the most general manifold with a metric g and a connection Γ , departures from Minkowski space are characterized by three geometrical entities: non-metricity (Q), curvature (R) and torsion

(S), defined as follows:

$$Q_{\mu\nu\rho} \equiv \nabla_{\mu}g_{\nu\rho}, \quad (1)$$

$$R^{\rho}{}_{\lambda\nu\mu} \equiv \Gamma^{\rho}{}_{\mu\lambda,\nu} - \Gamma^{\rho}{}_{\nu\lambda,\mu} + \Gamma^{\rho}{}_{\nu\alpha}\Gamma^{\alpha}{}_{\mu\lambda} - \Gamma^{\rho}{}_{\mu\alpha}\Gamma^{\alpha}{}_{\nu\lambda}, \quad (2)$$

$$S_{\mu\nu}{}^{\rho} \equiv \frac{1}{2}(\Gamma^{\rho}{}_{\mu\nu} - \Gamma^{\rho}{}_{\nu\mu}). \quad (3)$$

GR is the special case where the non-metricity and torsion are assumed to vanish identically ($Q = S = 0$, i.e., Riemann spacetime), which determines the connection in terms of the metric and leaves the metric as the only dynamical entity. However, as Figure 1 illustrates, this is by no means the only possibility, and many alternative geometric gravity theories have been discussed in the literature [20, 36–73] corresponding to alternative deforming geometries where other subsets of (Q, R, S) vanish. Embedding GR in a broader parametrized class of theories allowing non-vanishing torsion and non-metricity, and experimentally constraining these parameters would provide a natural generalization of the highly successful parametrized post-Newtonian (PPN) program for GR testing, which assumes vanishing torsion [1–3].

For the purposes of this paper, a particularly interesting generalization of Riemann spacetime is Riemann-Cartan Spacetime (also known as U_4), which retains $Q = 0$ but is characterized by non-vanishing torsion. In U_4 , torsion can be dynamical and consequently play a role in gravitation alongside the metric. Note that gravitation theories including torsion retain what are often regarded as the most beautiful aspects of General Relativity, i.e. general covariance and the idea that “gravity is geometry”. Torsion is just as geometrical an entity as curvature, and torsion theories can be consistent with the Weak Equivalence Principle (WEP).

*This is the “director’s cut” version of the article published in Phys. Rev. D November Issue, including extra bonus derivations in sections §II, §V and Appendix C.

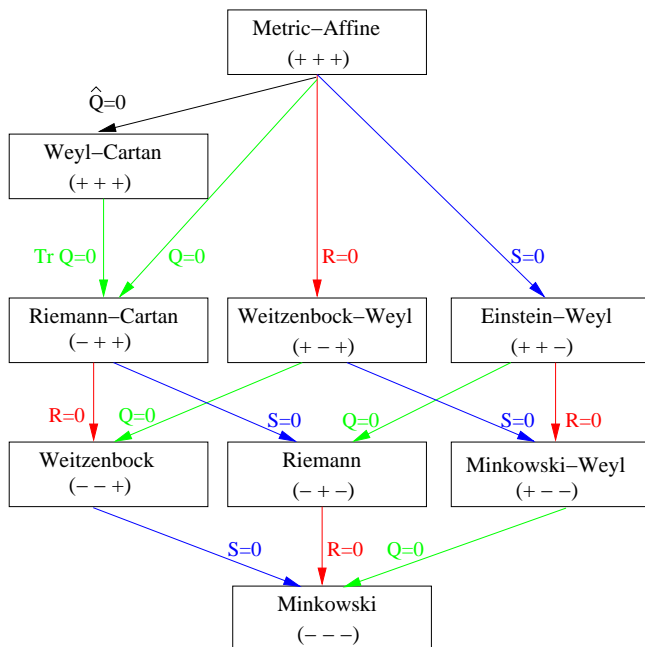


FIG. 1: Classification of spaces (Q,R,S) and the reduction flow. Metric-Affine spacetime is a manifold endowed with Lorentzian metric and linear affine connection without any restrictions. All spaces below it except the Weyl-Cartan space are special cases obtained from it by imposing three types of constraints: vanishing non-metricity tensor $Q_{\mu\nu\rho}$ (Q for short), vanishing Riemann curvature tensor $R_{\mu\nu\rho\sigma}$ (R for short), or vanishing torsion tensor $S_{\mu\nu}{}^\rho$ (S for short). A plus sign in a parenthesis indicates a non-vanishing quantity from the set (Q, R, S) , and a minus sign a vanishing quantity. For example, Riemann spacetime $(- + -)$ means that $Q = S = 0$ but $R \neq 0$. Weyl-Cartan space is a Metric-Affine space with vanishing “tracefree nonmetricity” $\hat{Q}_{\mu\nu\rho}$ (\hat{Q} for short), defined by $\hat{Q}_{\mu\nu\rho} \equiv Q_{\mu\nu\rho} - \frac{1}{4}(\text{tr}Q)_{\mu} g_{\nu\rho}$. The trace of the nonmetricity is defined by $(\text{tr}Q)_{\mu} \equiv g^{\nu\rho} Q_{\mu\nu\rho}$; thus \hat{Q} automatically satisfies that $(\text{tr}\hat{Q})_{\mu} = 0$ (tracefree). Subsets of the classification scheme are shown in Fig. 2 of [64], Fig. 1 of [30] and Fig. 5 of [38]. Among the terms, *Einstein-Weyl*, *Weitzenböck* and *Minkowski* spaces are standard, *Metric-Affine*, *Weyl-Cartan*, *Riemann-Cartan* and *Riemann* spaces follow [64], and we here introduce the terms *Weitzenböck-Weyl* and *Minkowski-Weyl* space by symmetry.

B. Why torsion testing is timely

Experimental searches for torsion have so far been rather limited [37], in part because most published torsion theories predict a negligible amount of torsion in the solar system. First of all, many torsion Lagrangians imply that torsion is related to its source via an algebraic equation rather than via a differential equation, so that (as opposed to curvature), torsion must vanish in vacuum. Second, even within the subset of torsion theories where torsion propagates and can exist in vacuum, it is usually assumed that it couples only to intrinsic spin, not to rotational angular momentum [42, 106, 107], and is therefore negligibly small far from extreme objects such as neutron stars. This second assumption also implies that even if torsion were present in the solar system, it would only affect particles with intrinsic spin (*e.g.* a gy-

roscope with net magnetic polarization) [106–108, 113–117], while having no influence on the precession of a gyroscope without nuclear spin [106–108] such as a gyroscope in Gravity Probe B.

Whether torsion does or does not satisfy these pessimistic assumptions depends on what the Lagrangian is, which is of course one of the things that should be tested experimentally rather than assumed. Taken at face value, the Hayashi-Shirafuji Lagrangian [75] provides an explicit counterexample to both assumptions, with even a static massive body generating a torsion field — indeed, such a strong one that the gravitational forces are due entirely to torsion, not to curvature. As another illustrative example, we will develop in Section IX a family of tetrad theories in Riemann-Cartan space which linearly interpolate between GR and the Hayashi-Shirafuji theory. Although these particular Lagrangians come with important caveats to which we return below (see also [126]), they show that one cannot dismiss out of hand the possibility that angular momentum sources non-local torsion (see also Table I). Note that the proof [106–108] of the oft-repeated assertion that a gyroscope without nuclear spin cannot feel torsion crucially relies on the assumption that orbital angular momentum cannot be the source of torsion. This proof is therefore not generally applicable in the context of non-standard torsion theories.

More generally, in the spirit of action=reaction, if a (non-rotating or rotating) mass like a planet can generate torsion, then a gyroscope without nuclear spin could be expected feel torsion, so the question of whether a non-standard gravitational Lagrangian causes torsion in the solar system is one which can and should be addressed experimentally.

This experimental question is timely because the Stanford-led gyroscope satellite experiment, Gravity Probe B¹ (GPB), was launched in April 2004 and has successfully been taking data. Preliminary GPB results, released in April 2007, have confirmed the geodetic precession to better than 1%, and the full results, which are highly relevant to this paper, are due to be released soon. GPB contains a set of four extremely spherical gyroscopes and flies in a circular polar orbit with altitude 640 kilometers, and we will show that it has the potential to severely constrain a broad class of previously allowed torsion theories. GPB was intended to test the GR prediction [76–81] that a gyroscope in this orbit precesses about 6,614.4 milli-arcseconds per year around its orbital angular momentum vector (geodetic precession) and about 40.9 milli-arcseconds per year about Earth’s angular momentum vector (frame-dragging)². Most impressively, GPB should convincingly observe the frame-dragging effect, an arguably still undetected effect of the

¹ <http://einstein.stanford.edu/>

² These numerical precession rates are taken from the GPB website.

Theory	Dynamical DOF	Vacuum	Source	Ref.	Notes
U_4 theory	$g_{\mu\nu}, S_{\mu\nu}^P$	N	Spin	[42]	
Pagels theory	$O(5)$ gauge fields ω_μ^{AB}	N	Spin	[128]	an $O(5)$ gauge theory of gravity
Metric-affine gravity	general gauge fields	P	Spin	[64]	gauge theory of gravity in the metric-affine space
Stelle-West	$SO(3,2)$ gauge fields ω_μ^{AB}	P	Spin, Gradient of the Higgs field	[127]	a $SO(3,2)$ gauge theory of gravity spontaneously broken to $SO(3,1)$
Hayashi-Shirafuji	tetrads e_μ^k	P	Spin, Rotational	[75]	a theory in Weitzenböck space
Einstein-Hayashi-Shirafuji	tetrads e_μ^k	P	Spin, Rotational	This paper	a class of theories in Riemann-Cartan space
Teleparallel gravity	tetrads e_μ^k	P	Spin, Rotational	[40, 41]	

TABLE I: A short list of torsion theories of gravity. The ‘‘DOF’’ in the second column is short for ‘‘degrees of freedom’’. In the column *Vacuum*, ‘‘N’’ refers to non-propagating torsion in the vacuum while ‘‘P’’ means propagating torsion. In the column *Source*, ‘‘spin’’ refers to intrinsic spin while ‘‘rotational’’ means rotational angular momentum.

off-diagonal metric elements that originate from the rotation of Earth. Of particular interest to us is that GPB can reach a precision of 0.005% for the geodetic precession, which as we will see enables precision discrimination³ between GR and a class of torsion theories.

C. How this paper is organized

In general, torsion has 24 independent components, each being a function of time and position. Fortunately, symmetry arguments and a perturbative expansion will allow us to greatly simplify the possible form of any torsion field of Earth, a nearly spherical slowly rotating massive object. We will show that the most general possibility can be elegantly parametrized by merely seven numerical constants to be constrained experimentally. We then derive the effect of torsion on the precession rate of a gyroscope in Earth orbit and work out how the anomalous precession that GPB would register depends on these seven parameters.

The rest of this paper is organized as follows. In Section II, we review the basics of Riemann-Cartan spacetime. In Section III, we derive the results of parametrizing the torsion field around Earth. In Section IV, we discuss the equation of motion for the precession of a gyroscope and the world-line of its center of mass. We use the results to calculate the instantaneous precession rate in Section V, and then analyze the Fourier moments for the particular orbit of GPB in Section VI. In Section VII, we show that GPB can constrain two linear combinations of the seven torsion parameters, given the constraints on the PPN parameters γ and α_1 from other solar system tests. To make our discussion less abstract, we study Hayashi-Shirafuji torsion gravity as an explicit illustra-

tive example of an alternative gravitational theory that can be tested within our framework. In Section VIII, we review the basics of Weitzenböck spacetime and Hayashi-Shirafuji theory, and then give the torsion-equivalent of the linearized Kerr solution. In Section IX, we generalize the Hayashi-Shirafuji theory to a two-parameter family of gravity theories, which we will term Einstein-Hayashi-Shirafuji (EHS) theories, interpolating between torsion-free GR and the Hayashi-Shirafuji maximal torsion theory. In Section X, we apply the precession rate results to the EHS theories and discuss the observational constraints that GPB, alongside other solar system tests, will be able to place on the parameter space of the family of EHS theories. We conclude in Section XI. Technical details of torsion parametrization (i.e. Section III) are given in Appendices A & B. Derivation of solar system tests are given in Appendix C. We also demonstrate in Appendix D that current ground-based experimental upper bounds on the photon mass do not place more stringent constraints on the torsion parameters t_1 or t_2 than GPB will.

After the first version of this paper was submitted, Flanagan and Rosenthal showed that the Einstein-Hayashi-Shirafuji Lagrangian has serious defects [126], while leaving open the possibility that there may be other viable Lagrangians in the same class (where spinning objects generate and feel propagating torsion). The EHS Lagrangian should therefore not be viewed as a viable physical model, but as a pedagogical toy model giving concrete illustrations of the various effects and constraints that we discuss.

Throughout this paper, we use natural gravitational units where $c = G = 1$. Unless we explicitly state otherwise, a Greek letter denotes an index running from 0 to 3 and a Latin letter an index from 1 to 3. We use the metric signature convention $(-+++)$.

³ GPB also has potential for constraining other GR extensions [82] than those we consider in this paper.

II. RIEMANN-CARTAN SPACETIME

We review the basics of Riemann-Cartan spacetime only briefly here, and refer the interested reader to Hehl *et al.* [42] for a more comprehensive discussion of spacetime with torsion. Riemann-Cartan spacetime is a connected C^∞ four-dimensional manifold endowed with metric $g_{\mu\nu}$ of Lorentzian signature and an affine connection $\Gamma^\mu_{\nu\rho}$ such that the non-metricity defined by Eq. (1) with respect to the full connection identically vanishes. In other words, the connection in Riemann-Cartan spacetime may have torsion, but it must still be compatible with the metric ($g_{\mu\nu;\lambda} = 0$). The covariant derivative of a vector is given by

$$\nabla_\mu V^\nu = \partial_\mu V^\nu + \Gamma^\nu_{\mu\rho} V^\rho, \quad (4)$$

$$\nabla_\mu V_\nu = \partial_\mu V_\nu - \Gamma^\rho_{\mu\nu} V_\rho, \quad (5)$$

where the first of the lower indices on $\Gamma^\lambda_{\mu\sigma}$ always corresponds to the index on ∇_μ .

The full connection has 64 independent components. The condition of vanishing non-metricity $\nabla_\mu g_{\nu\rho} = 0$ gives 40 constraints, and the remaining 24 components are the degrees of freedom of the torsion tensor.

In the more familiar case of Riemann spacetime, the two conditions $S_{\mu\nu}{}^\rho = 0$ and $Q_{\mu\nu\rho} = 0$ imply that the connection must be the so-called Levi-Civita connection (Christoffel symbol), uniquely determined by the metric as

$$\left\{ \begin{array}{c} \rho \\ \mu\nu \end{array} \right\} = \frac{1}{2} g^{\rho\lambda} (\partial_\mu g_{\nu\lambda} + \partial_\nu g_{\mu\lambda} - \partial_\lambda g_{\mu\nu}). \quad (6)$$

In the more general case when torsion is present, the connection must depart from the Levi-Civita connection in order to be metric-compatible ($\nabla_\mu g_{\nu\rho} = 0$), and this departure is (up to a historical minus sign) called the *contorsion*, defined as

$$K_{\mu\nu}{}^\rho \equiv \left\{ \begin{array}{c} \rho \\ \mu\nu \end{array} \right\} - \Gamma^\rho_{\mu\nu}. \quad (7)$$

Using the fact that the torsion is the part of the connection that is antisymmetric in the first two indices (Eq. 3), one readily shows that

$$K_{\mu\nu}{}^\rho = -S_{\mu\nu}{}^\rho - S^\rho_{\nu\mu} - S^\rho_{\mu\nu}. \quad (8)$$

In Riemann-Cartan spacetime, the metric is used to raise or lower the indices as usual.

The curvature tensor is defined as usual, in terms of the full connection rather than the Levi-Civita connection:

$$R^\rho_{\lambda\nu\mu} = \partial_\nu \Gamma^\rho_{\mu\lambda} - \partial_\mu \Gamma^\rho_{\nu\lambda} + \Gamma^\rho_{\nu\alpha} \Gamma^\alpha_{\mu\lambda} - \Gamma^\rho_{\mu\alpha} \Gamma^\alpha_{\nu\lambda}. \quad (9)$$

As in Riemann spacetime, one can prove that $R^\rho_{\lambda\nu\mu}$ is a tensor by showing that for any vector V^μ ,

$$\nabla_{[\nu} \nabla_{\mu]} V^\rho = \frac{1}{2} R^\rho_{\lambda\nu\mu} V^\lambda - S_{\nu\mu}{}^\alpha \nabla_\alpha V^\rho. \quad (10)$$

The Ricci tensor and Ricci scalar are defined by contraction the Riemann tensor just as in Riemann spacetime.

III. PARAMETRIZATION OF THE TORSION AND CONNECTION

The torsion tensor has twenty-four independent components since it is antisymmetric in its first two indices. However, its form can be greatly simplified by the fact that Earth is well approximated as a uniformly rotating spherical object. Throughout this paper, we will therefore Taylor expand all quantities with respect to the dimensionless mass parameter

$$\varepsilon_m \equiv \frac{m}{r}, \quad (11)$$

and the dimensionless angular momentum parameter

$$\varepsilon_a \equiv \frac{a}{r}, \quad (12)$$

where $a \equiv J/m$ is the specific angular momentum, which has units of length, and r is the distance of the field point from the central gravitating body. Here m and J are Earth's mass and rotational angular momentum, respectively. Since Earth is slowly rotating ($\varepsilon_a \ll 1$), we will only need to keep track of zeroth and first order terms in ε_a . We will also Taylor expand with respect to ε_m to first order, since we are interested in objects with orbital radii vastly exceeding Earth's Schwarzschild radius ($\varepsilon_m \ll 1$).⁴ All calculations will be to first order in ε_m , because to zeroth order in ε_m , i.e. in Minkowski spacetime, there is no torsion. Consequently, we use the terms "zeroth order" and "first order" below with respect to the expansion in ε_a .

We start by studying in section III A the zeroth order part: the static, spherically and parity symmetric case where Earth's rotation is ignored. The first correction will be treated in section III B: the stationary and spherically axisymmetric contribution caused by Earth's rotation. For each case, we start by giving the symmetry constraints that apply for *any* quantity. We then give the most general parametrization of torsion and connection that is consistent with these symmetries, as derived in the appendices. The Kerr-like torsion solution of Hayashi-Shirafuji Lagrangian given in Section VIII is an explicit example within this parametrized class. In Section V, we will apply these results to the precession of a gyroscope around Earth.

A. Zeroth order: the static, spherically and parity symmetric case

This is the order at which Earth's slow rotation is neglected ($\varepsilon_a = 0$). For this, three convenient coordinate

⁴ These two approximations $\varepsilon_m \ll 1$ and $\varepsilon_a \ll 1$ are highly accurate for the GPB satellite in an Earth orbit with altitude about 640 kilometers: $\varepsilon_m \simeq 6.3 \times 10^{-10}$ and $\varepsilon_a \simeq 5.6 \times 10^{-7}$.

systems are often employed – isotropic rectangular coordinates, isotropic spherical coordinates, and standard spherical coordinates. In the following, we will find it most convenient to work in isotropic rectangular coordinates to set up and solve the problem, and then transform the result to standard spherical coordinates.

1. Symmetry Principles

Tetrad spaces with spherical symmetry have been studied by Robertson [118] and Hayashi and Shirafuji [75]. Our approach in this section essentially follows their work.

Given spherical symmetry, one can naturally find a class of isotropic rectangular coordinates (t, x, y, z) . Consider a general quantity $\mathcal{O}(x)$ that may bear upper and lower indices. It may or may not be a tensor. In either case, its transformation law $\mathcal{O}(x) \rightarrow \mathcal{O}'(x')$ under the general coordinate transformation $x \rightarrow x'$ should be given. By definition, a quantity \mathcal{O} is static, spherically and parity symmetric if it has the *formal functional invariance*

$$\mathcal{O}'(x') = \mathcal{O}(x')$$

under the following coordinate transformations (note that $\mathcal{O}(x')$ denotes the original function $\mathcal{O}(x)$ evaluated at the coordinates x'):

1. Time translation: $t \rightarrow t' \equiv t + t_0$ where t_0 is an arbitrary constant.
2. Time reversal: $t \rightarrow t' \equiv -t$.
3. Continuous rotation and space inversion:

$$\mathbf{x} \rightarrow \mathbf{x}' \equiv \mathbf{R}\mathbf{x}, \quad (13)$$

where \mathbf{R} is any 3×3 constant orthogonal ($\mathbf{R}^t \mathbf{R} = \mathbf{I}$) matrix. Note that the parity symmetry allows \mathbf{R} to be an improper rotation.

2. Parametrization of torsion

It can be shown (see Appendix A) that, under the above conditions, there are only two independent components of the torsion tensor. The non-zero torsion components can be parametrized in isotropic rectangular coordinates as follows:

$$S_{0i}{}^0 = t_1 \frac{m}{2r^3} x^i, \quad (14)$$

$$S_{jk}{}^i = t_2 \frac{m}{2r^3} (x^j \delta_{ki} - x^k \delta_{ji}), \quad (15)$$

where t_1 and t_2 are dimensionless constants. It is of course only the two combinations $t_1 m$ and $t_2 m$ that correspond to the physical parameters; we have chosen to introduce a third redundant quantity m here, with units

of mass, to keep t_1 and t_2 dimensionless. Below we will see that in the context of specific torsion Lagrangians, m can be naturally identified with the mass of the object generating the torsion, up to a numerical factor close to unity.

We call t_1 the “anomalous geodetic torsion” and t_2 the “normal geodetic torsion”, because both will contribute to the geodetic spin precession of a gyroscope, the former “anomalously” and the latter “regularly”, as will become clear in Section V and VI.

3. Torsion and connection in standard spherical coordinates

In spherical coordinates, the torsion tensor has the following non-vanishing components:

$$S_{tr}{}^t(r) = t_1 \frac{m}{2r^2}, \quad S_{r\theta}{}^\theta(r) = S_{r\phi}{}^\phi(r) = t_2 \frac{m}{2r^2}, \quad (16)$$

where t_1 and t_2 are the same torsion constants as defined above.

The above parametrization of torsion was derived in isotropic coordinates, but it is also valid in other spherical coordinates as far as the linear perturbation around the Minkowski spacetime is concerned. The decomposition formula (Eq. 7), derived from $\nabla_\mu g_{\nu\rho} = 0$, enables one to calculate the full connection exactly. However, for that purpose the coordinates with a metric must be specified. In general, a spherically symmetric coordinate system has the line element [83]

$$ds^2 = -h(r)dt^2 + f(r)dr^2 + \alpha(r)r^2 [d\theta^2 + \sin^2 \theta d\phi^2].$$

There is freedom to rescale the radius, so-called isotropic spherical coordinates corresponding to the choice $\alpha(r) = f(r)$. Throughout this paper, we make the common choice $\alpha(r) = 1$, where r can be interpreted as $(2\pi)^{-1}$ times the circumference of a circle. To linear order,

$$h(r) = 1 + \mathcal{H} \frac{m}{r},$$

$$f(r) = 1 + \mathcal{F} \frac{m}{r},$$

where \mathcal{H} and \mathcal{F} are dimensionless constants.

It is straightforward to show that, in the linear regime, the most general connection that is static, spherically and parity symmetric in Riemann-Cartan spacetime with

standard spherical coordinates is as follows:

$$\begin{aligned}
\Gamma^t{}_{tr} &= \left(t_1 - \frac{\mathcal{H}}{2}\right) \frac{m}{r^2}, \\
\Gamma^t{}_{rt} &= -\frac{\mathcal{H}m}{2r^2}, \\
\Gamma^r{}_{tt} &= \left(t_1 - \frac{\mathcal{H}}{2}\right) \frac{m}{r^2}, \\
\Gamma^r{}_{rr} &= -\frac{\mathcal{F}m}{2r^2}, \\
\Gamma^r{}_{\theta\theta} &= -r + (\mathcal{F} + t_2)m, \\
\Gamma^r{}_{\phi\phi} &= -r \sin^2 \theta + (\mathcal{F} + t_2)m \sin^2 \theta, \\
\Gamma^\theta{}_{r\theta} &= \Gamma^\phi{}_{r\phi} = \frac{1}{r}, \\
\Gamma^\theta{}_{\theta r} &= \Gamma^\phi{}_{\phi r} = \frac{1}{r} - t_2 \frac{m}{r^2}, \\
\Gamma^\theta{}_{\phi\phi} &= -\sin \theta \cos \theta, \\
\Gamma^\phi{}_{\theta\phi} &= \Gamma^\phi{}_{\phi\theta} = \cot \theta.
\end{aligned} \tag{17}$$

By ‘‘the most general’’ we mean that any other connections are related to the one in Eq. (17) by the nonlinear coordinate transformation law

$$\Gamma'^\mu{}_{\nu\lambda}(x') = \frac{\partial x'^\mu}{\partial x^\alpha} \frac{\partial x^\beta}{\partial x'^\nu} \frac{\partial x^\gamma}{\partial x'^\lambda} \Gamma^\alpha{}_{\beta\gamma}(x) + \frac{\partial x'^\mu}{\partial x^\alpha} \frac{\partial^2 x^\alpha}{\partial x'^\nu \partial x'^\lambda}. \tag{18}$$

Note that the terms independent of metric and torsion merely reflect the spherical coordinate system and do not represent a deformation of spacetime — in other words, the special case $t_1 = t_2 = \mathcal{H} = -\mathcal{F} = 0$ corresponds to the connection for Minkowski spacetime. The case $t_1 = t_2 = 0$ and $\mathcal{H} = -\mathcal{F} = -2$ corresponds to the standard connection for Schwarzschild spacetime in the linear regime ($r \gg m$).

B. First-order: stationary, spherically axisymmetric case

The terms added at this order are due to Earth’s rotation. Roughly speaking, ‘‘spherically axisymmetric’’ refers to the property that a system is spherically symmetric except for symmetries broken by an angular momentum vector. The rigorous mathematical definition is given in Section III B 1. Subtleties related to coordinate system choices at this order fortunately do not matter in the $\varepsilon_m \ll 1$ and $\varepsilon_a \ll 1$ limit that we are interested in.

1. Symmetry Principles

Suppose we have a field configuration which depends explicitly on the angular momentum \mathbf{J} of the central spinning body. We can denote the fields generically as $\mathcal{O}(x|\mathbf{J})$, which is a function of coordinates x and the value of the angular momentum vector \mathbf{J} . We assume

that the underlying laws of physics are symmetric under rotations, parity, time translation, and time reversal, so that the field configurations for various values of \mathbf{J} can be related to each other. Specifically, we assume that \mathbf{J} rotates as a vector, reverses under time-reversal, and is invariant under time translation and parity. It is then possible to define transformations for the field configurations, $\mathcal{O}(x|\mathbf{J}) \rightarrow \mathcal{O}'(x'|\mathbf{J})$, for these same symmetry operations. Here $\mathcal{O}'(x'|\mathbf{J})$ denotes the transform of the field configuration that was specified by \mathbf{J} before the transformation; \mathcal{O} may or may not be a tensor, but its transformation properties are assumed to be specified. The symmetries of the underlying laws of physics then imply that the configurations $\mathcal{O}(x|\mathbf{J})$ are stationary and *spherically axisymmetric* in the sense that the transformed configuration is identical to the configuration that one would compute by transforming $\mathbf{J} \rightarrow \mathbf{J}'$. That is,

$$\mathcal{O}'(x'|\mathbf{J}) = \mathcal{O}(x'|\mathbf{J}')$$

under the following coordinate transformations:

1. time translation: $t \rightarrow t' \equiv t + t_0$ where t_0 is an arbitrary constant.
2. Time reversal: $t \rightarrow t' \equiv -t$.
3. Continuous rotation and space inversion: $\mathbf{x} \rightarrow \mathbf{x}' \equiv \mathbf{R}(\mathbf{x})$, i.e. \mathbf{x}' is related to \mathbf{x} by any proper or improper rotation.

Below we will simplify the problem by keeping track only of terms linear in $J/r^2 = \varepsilon_m \varepsilon_a$.

2. Parametrization of metric

With these symmetries, it can be shown that the first-order contribution to the metric is

$$g_{ti} = g_{it} = \frac{\mathcal{G}}{r^2} \epsilon_{ijk} J^j \hat{x}^k \tag{19}$$

in rectangular coordinates $x^\mu = (t, x^i)$, where \mathcal{G} is a constant, or

$$g_{t\phi} = g_{\phi t} = \mathcal{G} \frac{J}{r} \sin^2 \theta \tag{20}$$

in spherical coordinates $x^\mu = (t, r, \theta, \phi)$ where the polar angle θ is the angle with respect to the rotational angular momentum \mathbf{J} . The details of the derivation are given in Appendix B.

3. Parametrization of torsion

In Appendix B, we show that, in rectangular coordinates, the first-order correction to the torsion is

$$\begin{aligned}
S_{ij}{}^t &= \frac{f_1}{2r^3} \epsilon_{ijk} J^k + \frac{f_2}{2r^3} J^k \hat{x}^l (\epsilon_{ikl} \hat{x}^j - \epsilon_{jkl} \hat{x}^i), \\
S_{tij} &= \frac{f_3}{2r^3} \epsilon_{ijk} J^k + \frac{f_4}{2r^3} J^k \hat{x}^l \epsilon_{ikl} \hat{x}^j + \frac{f_5}{2r^3} J^k \hat{x}^l \epsilon_{jkl} \hat{x}^i.
\end{aligned}$$

In spherical coordinates, these first-order torsion terms are

$$\begin{aligned}
S_{r\phi}{}^t &= w_1 \frac{ma}{2r^2} \sin^2 \theta, \\
S_{\theta\phi}{}^t &= w_2 \frac{ma}{2r} \sin \theta \cos \theta, \\
S_{t\phi}{}^r &= w_3 \frac{ma}{2r^2} \sin^2 \theta, \\
S_{t\phi}{}^\theta &= w_4 \frac{ma}{2r^3} \sin \theta \cos \theta, \\
S_{tr}{}^\phi &= w_5 \frac{ma}{2r^4}, \\
S_{t\theta}{}^\phi &= -w_4 \frac{ma}{2r^3} \cot \theta.
\end{aligned}$$

Here f_1, \dots, f_5 and w_1, \dots, w_5 are constants. The latter are linear combinations of the former. The details of the derivation are given in Appendix B. We call w_1, \dots, w_5 the ‘‘frame-dragging torsion’’, since they will contribute the frame-dragging spin precession of a gyroscope as will become clear in Section V.

C. Around Earth

We now summarize the results to linear order. We have computed the parametrization perturbatively in the dimensionless parameters $\varepsilon_m \equiv m/r$ and $\varepsilon_a \equiv a/r$. The zeroth order ($\varepsilon_a = 0$) solution, where Earth’s slow rotation is ignored, is simply the solution around a static spherical body, i.e. the case studied in Section III A. The first order correction, due to Earth’s rotation, is stationary and spherically axisymmetric as derived in Section III B. A quantity \mathcal{O} to linear order is the sum of these two orders. In spherical coordinates, a general line element thus takes the form

$$\begin{aligned}
ds^2 &= - \left[1 + \mathcal{H} \frac{m}{r} \right] dt^2 + \left[1 + \mathcal{F} \frac{m}{r} \right] dr^2 + \\
&\quad + r^2 d\Omega^2 + 2 \mathcal{G} \frac{ma}{r} \sin^2 \theta dt d\phi,
\end{aligned} \tag{21}$$

where $d\Omega^2 = d\theta^2 + \sin^2 \theta d\phi^2$. Here \mathcal{H} , \mathcal{F} and \mathcal{G} are dimensionless constants. In GR, the Kerr metric [84, 85] at large distance gives the constants $\mathcal{H} = -\mathcal{F} = \mathcal{G} = -2$. The result $\mathcal{G} = -2$ can also be derived more generally as shown by de Sitter [86] and Lense & Thirring [87]. As above, $J = ma$ denotes the magnitude of Earth’s rotational angular momentum.

Combining our 0th and 1st order expressions from

above for the torsion around Earth, we obtain

$$\begin{aligned}
S_{tr}{}^t &= t_1 \frac{m}{2r^2}, \\
S_{r\theta}{}^\theta &= S_{r\phi}{}^\phi = t_2 \frac{m}{2r^2}, \\
S_{r\phi}{}^t &= w_1 \frac{ma}{2r^2} \sin^2 \theta, \\
S_{\theta\phi}{}^t &= w_2 \frac{ma}{2r} \sin \theta \cos \theta, \\
S_{t\phi}{}^r &= w_3 \frac{ma}{2r^2} \sin^2 \theta, \\
S_{t\phi}{}^\theta &= w_4 \frac{ma}{2r^3} \sin \theta \cos \theta, \\
S_{tr}{}^\phi &= w_5 \frac{ma}{2r^4}, \\
S_{t\theta}{}^\phi &= -w_4 \frac{ma}{2r^3} \cot \theta.
\end{aligned} \tag{22}$$

All other components vanish. Again, $t_1, t_2, w_1, w_2, w_3, w_4, w_5$ are dimensionless constants.

The calculation of the corresponding connection is straightforward by virtue of Eq. (7). It is not hard to show that, to linear order in a Riemann-Cartan spacetime in spherical coordinates, the connection around Earth has the following non-vanishing components:

$$\begin{aligned}
\Gamma^t{}_{tr} &= \left(t_1 - \frac{\mathcal{H}}{2} \right) \frac{m}{r^2}, \\
\Gamma^t{}_{rt} &= -\frac{\mathcal{H} m}{2 r^2}, \\
\Gamma^t{}_{r\phi} &= (3\mathcal{G} + w_1 - w_3 - w_5) \frac{ma}{2r^2} \sin^2 \theta, \\
\Gamma^t{}_{\phi r} &= (3\mathcal{G} - w_1 - w_3 - w_5) \frac{ma}{2r^2} \sin^2 \theta, \\
\Gamma^t{}_{\theta\phi} &= w_2 \frac{ma}{2r} \sin \theta \cos \theta, \\
\Gamma^t{}_{\phi\theta} &= -w_2 \frac{ma}{2r} \sin \theta \cos \theta, \\
\Gamma^r{}_{tt} &= \left(t_1 - \frac{\mathcal{H}}{2} \right) \frac{m}{r^2}, \\
\Gamma^r{}_{rr} &= -\frac{\mathcal{F} m}{2 r^2}, \\
\Gamma^r{}_{\theta\theta} &= -r + (\mathcal{F} + t_2)m, \\
\Gamma^r{}_{\phi\phi} &= -r \sin^2 \theta + (\mathcal{F} + t_2)m \sin^2 \theta, \\
\Gamma^r{}_{t\phi} &= (\mathcal{G} - w_1 + w_3 - w_5) \frac{ma}{2r^2} \sin^2 \theta, \\
\Gamma^r{}_{\phi t} &= (\mathcal{G} - w_1 - w_3 - w_5) \frac{ma}{2r^2} \sin^2 \theta, \\
\Gamma^\theta{}_{t\phi} &= (-2\mathcal{G} - w_2 + 2w_4) \frac{ma}{2r^3} \sin \theta \cos \theta, \\
\Gamma^\theta{}_{\phi t} &= (-2\mathcal{G} - w_2) \frac{ma}{2r^3} \sin \theta \cos \theta, \\
\Gamma^\theta{}_{r\theta} &= \Gamma^\phi{}_{r\phi} = \frac{1}{r}, \\
\Gamma^\theta{}_{\theta r} &= \Gamma^\phi{}_{\phi r} = \frac{1}{r} - t_2 \frac{m}{r^2},
\end{aligned} \tag{23}$$

$$\begin{aligned}
\Gamma_{\phi\phi}^{\theta} &= -\sin\theta \cos\theta, \\
\Gamma_{tr}^{\phi} &= (-\mathcal{G} + w_1 - w_3 + w_5) \frac{ma}{2r^4}, \\
\Gamma_{rt}^{\phi} &= (-\mathcal{G} + w_1 - w_3 - w_5) \frac{ma}{2r^4}, \\
\Gamma_{t\theta}^{\phi} &= (2\mathcal{G} + w_2 - 2w_4) \frac{ma}{2r^3} \cot\theta, \\
\Gamma_{\theta t}^{\phi} &= (2\mathcal{G} + w_2) \frac{ma}{2r^3} \cot\theta, \\
\Gamma_{\theta\phi}^{\phi} &= \Gamma_{\phi\theta}^{\phi} = \cot\theta.
\end{aligned}$$

IV. PRECESSION OF A GYROSCOPE I: FUNDAMENTALS

A. Rotational angular momentum

There are two ways to covariantly quantify the angular momentum of a spinning object, in the literature denoted S^μ and $S^{\mu\nu}$, respectively. (Despite our overuse of the letter S , they can be distinguished by the number of indices.) In the rest frame of the center of mass of a gyroscope, the 4-vector S^μ is defined as

$$S^\mu = (0, \vec{S}_0), \quad (24)$$

and the 4-tensor $S^{\mu\nu}$ is defined to be antisymmetric and have the components

$$S^{0i} = S^{i0} = 0, \quad S^{ij} = \epsilon^{ijk} S_0^k, \quad (25)$$

where $i = x, y, z$. $\vec{S}_0 = S_0^x \hat{x} + S_0^y \hat{y} + S_0^z \hat{z}$ is the rotational angular momentum of a gyroscope observed by an observer co-moving with the center of mass of the gyroscope. The relation between S^μ and $S^{\mu\nu}$ can be written in the local (flat) frame as

$$S^\mu = \epsilon^{\mu\nu\rho\sigma} u_\nu S_{\rho\sigma}, \quad (26)$$

where $u^\mu = dx^\mu/d\tau$ is the 4-velocity.

In curved spacetime, the Levi-Civita symbol is generalized to $\bar{\epsilon}^{\mu\nu\rho\sigma} = \epsilon^{\mu\nu\rho\sigma}/\sqrt{-g}$ where $g = \det g_{\mu\nu}$. It is easy to prove that $\bar{\epsilon}^{\mu\nu\rho\sigma}$ is a 4-tensor. Then Eq. (26) becomes a covariant relation

$$S^\mu = \bar{\epsilon}^{\mu\nu\rho\sigma} u_\nu S_{\rho\sigma}. \quad (27)$$

In addition, the vanishing of temporal components of S^μ and $S^{\mu\nu}$ can be written as covariant conditions as follows:

$$S^\mu u_\mu = 0, \quad (28)$$

$$S^{\mu\nu} u_\nu = 0. \quad (29)$$

In the literature [76], Eq. (29) is called Pirani's supplementary condition.

Note, however, that unlike the flat space case, the spatial vectors of S^μ and $S^{\mu\nu}$ (denoted by \vec{S} and \vec{S}' respectively) do not coincide in the curved spacetime. The former is the spatial component of the 4-vector

S^μ , while the latter is historically defined as $\vec{S}'^i \equiv \epsilon^{ijk} S_{jk}$. It follows Eq. (27) that \vec{S} and \vec{S}' differ by $\vec{S} = \vec{S}' [1 + \mathcal{O}(m_E/r) + \mathcal{O}(v^2)]$ for a gyroscope moving around Earth.

B. Equation of motion for precession of a gyroscope

To derive the equation of motion for S^μ (or $S^{\mu\nu}$) of a small extended object that may have either rotational angular momentum or net spin, Papapetrou's method [120] should be generalized to Riemann-Cartan spacetime. This generalization has been studied by Stoeger & Yasskin [106, 107] as well as Nomura, Shirafuji & Hayashi [108]. The starting point of this method is the Bianchi identity or Noether current in a gravitational theory whose derivation strongly relies on an assumption of what sources torsion. Under the common assumption that only intrinsic spin sources torsion, both [106, 107] and [108] drew the conclusion that whereas a particle with net intrinsic spin will precess according to the full connection, the rotational angular momentum of a gyroscope will *not* feel the background torsion, i.e. it will undergo parallel transport by the Levi-Civita connection along the free-falling orbit — the same prediction as in GR.

These results of [106–108] have the simple intuitive interpretation that if angular momentum is not coupled to torsion, then torsion is not coupled to angular momentum. In other words, for Lagrangians where the angular momentum of a rotating object cannot generate a torsion field, the torsion field cannot affect the angular momentum of a rotating object, in the same spirit as Newton's dictum “action = reaction”.

The Hayashi-Shirafuji theory of gravity, which we will discuss in detail in Section VIII, raises an objection to the common assumption that only intrinsic spin sources torsion, in that in this theory even a non-rotating massive body can generate torsion in the vacuum nearby [75]. This feature also generically holds for teleparallel theories. It has been customary to assume that spinless test particles follow metric geodesics (have their momentum parallel transported by the Levi-Civita connection), i.e. that spinless particles decouple from the torsion even if it is nonzero. For a certain class of Lagrangians, this can follow from using the conventional variational principle. However, Kleinert and Pelster [109, 110] argue that the closure failure of parallelograms in the presence of torsion adds an additional term to the geodesics which causes spinless test particles to follow autoparallel worldlines (have their momentum parallel transported by the full connection). This scenario thus respects the “action = reaction” principle, since a spinless test particle can both generate and feel torsion. As a natural extension, we explore the possibility that in these theories, a rotating body also generates torsion through its rotational angular momentum, and the torsion in turn affects the

motion of spinning objects such as gyroscopes.

An interesting first-principles derivation of how torsion affects a gyroscope in a specific theory might involve generalizing the matched asymptotic expansion method of [111, 112], and match two generalized Kerr-solutions in the weak-field limit to obtain the gyroscope equation of motion. Since such a calculation would be way beyond the scope of the present paper, we will simply limit our analysis to exploring some obvious possibilities for laws of motion, based on the analogy with spin precession.

The exact equation of motion for the precession of net spin is model dependent, depending on the way the matter fields couple to the metric and torsion in the Lagrangian (see [106–108, 113–117, 121]). However, in the linear regime that we are interested in here, many of the cases reduce to one of the following two equations if there is no external non-gravitational force acting on the test particle:

$$\frac{DS^\mu}{D\tau} = 0, \quad (30)$$

$$\text{or } \frac{DS^{\mu\nu}}{D\tau} = 0, \quad (31)$$

where $D/D\tau = (dx^\mu/d\tau)\nabla_\mu$ is the covariant differentiation along the world-line with respect to the full connection. In other words, the net spin undergoes parallel transport by the full connection along its trajectory.⁵

In analog to the precession of spin, we will work out the implications of the assumption that the rotational angular momentum also precesses by parallel transport along the free-fall trajectory using the full connection.

C. World line of the center of mass

In GR, test particles move along well-defined trajectories – *geodesics*. In the presence of torsion, things might be different. The idea of *geodesics* originates from two independent concepts: *autoparallels* and *extremals*⁶. Autoparallels, or affine geodesics, are curves along which the velocity vector $dx^\mu/d\lambda$ is transported parallel to itself by the full connection $\Gamma^\rho_{\mu\nu}$. With an affine parameter λ , the geodesic equation is

$$\frac{d^2x^\rho}{d\lambda^2} + \Gamma^\rho_{(\mu\nu)} \frac{dx^\mu}{d\lambda} \frac{dx^\nu}{d\lambda} = 0. \quad (32)$$

Extremals, or metric geodesics, are curves of extremal spacetime interval with respect to the metric $g_{\mu\nu}$. Since $ds = [-g_{\mu\nu}(x)dx^\mu dx^\nu]^{1/2}$ does not depend on the full connection, the geodesic differential equations derived

from $\delta \int ds = 0$ state that the 4-vector is parallel transported by the Levi-Civita connection. That is, with the parameter λ properly chosen,

$$\frac{d^2x^\rho}{d\lambda^2} + \left\{ \begin{array}{c} \rho \\ \mu\nu \end{array} \right\} \frac{dx^\mu}{d\lambda} \frac{dx^\nu}{d\lambda} = 0. \quad (33)$$

In Riemann spacetime where torsion identically vanishes, Eqs.(32) and (33) coincide. In a Riemann-Cartan spacetime, however, these two curves coincide if and only if the torsion is totally antisymmetric in all three indices [42]. This is because the symmetric part of the full connection can be written from Eq. (7) as follows:

$$\Gamma^\rho_{(\mu\nu)} \equiv \frac{1}{2}(\Gamma^\rho_{\mu\nu} + \Gamma^\rho_{\nu\mu}) = \left\{ \begin{array}{c} \rho \\ \mu\nu \end{array} \right\} + S^\rho_{\mu\nu} + S^\rho_{\nu\mu}. \quad (34)$$

Photons are expected to follow extremal world lines because the gauge invariance of the electromagnetic part of the Lagrangian, well established by numerous experimental upper bounds on the photon mass, prohibits torsion from coupling to the electromagnetic field to lowest order [42]. As a consequence, the classical path of a light ray is at least to leading order determined by the metric alone as an extremal path, or equivalently as an autoparallel curve with respect to the Levi-Civita connection, independent of whether there is torsion.

On the other hand, the trajectory of a rotating test particle is still an open question in theory. Papapetrou [120] claims that, even in GR, a gyroscope will deviate from the metric geodesic, albeit slightly. In torsion gravity theories, the equations of motion for the orbital 4-momentum differs more strongly between different approaches [42, 107, 108, 113–117], and it is an open question to what extent they are consistent with all classical GR tests (deflection of light rays, gravitational redshift, precession of the perihelion of Mercury, Shapiro time delay, binary pulsars, etc.). To bracket the uncertainty, we will examine the two extreme assumption in turn – that world lines are autoparallels and extremals, respectively.

Only the autoparallel scheme, not the extremal scheme, is theoretically consistent, for two reasons. The first reason is based on the equivalence of the two approaches using the two alternative quantities S^μ and $S^{\mu\nu}$ to describe the angular momentum. The equivalence is automatic in GR. In a torsion theory, however, Eq. (30) and (31) can be simultaneously valid only if the trajectory is autoparallel. This can be seen by taking the covariant differentiation of Eq. (27). Note that $D\bar{\epsilon}^{\mu\nu\rho\sigma}/D\tau = 0$. One finds

$$\bar{\epsilon}^{\mu\nu\rho\sigma} \frac{Du_\nu}{D\tau} S_{\rho\sigma} = 0. \quad (35)$$

This equation is satisfied if $Du_\nu/D\tau = 0$, i.e. if the gyroscope world line is autoparallel. If an extremal world line is assumed, then one has to make an *a priori* choice between S^μ and $S^{\mu\nu}$, since the precession rates calculated using the two quantities will differ.

⁵ If an external non-gravitational force acts on a spinning test particle, it will undergo Fermi-Walker transport along its world-line. This situation is beyond the interest of a satellite experiment, so it will be neglected in the present paper.

⁶ This terminology follows Hehl *et al.* [42].

The second reason is that for S^μ , the condition $S^\mu u_\mu = 0$ (Eq. (28)) must be satisfied anywhere along the world line. Taking the covariant differentiation for both sides of Eq. (28), one finds

$$S^\mu D u_\mu / D\tau = 0, \quad (36)$$

assuming $DS^\mu/D\tau = 0$. Obviously, autoparallels are consistent with Eq. (36), while extremals are not. The same argument applies for $S^{\mu\nu}$, i.e. taking the covariant differentiation of both sides of Eq. (29).

Despite the fact that the extremal scheme is not theoretically consistent in this sense, the inconsistencies are numerically small for the linear regime $m/r \ll 1$. They are therefore of interest as an approximate phenomenological prescription that might at some time in the future be incorporated into a consistent theory. We therefore include results also for this case below.

D. Newtonian limit

In Section III, we parametrized the metric, torsion and connection of Earth, including an arbitrary parameter m with units of mass. To give m a physical interpretation, the Newtonian limit of a test particle's orbit should be evaluated. Obviously, the result depends on whether the autoparallel or extremal scheme is assumed.

In the remainder of this paper, we denote an arbitrary parameter with units of mass as m_0 and the physical mass as m . Metric and torsion parameters in accordance with m_0 are denoted with a superscript (0), i.e. $\mathcal{H}^{(0)}, \mathcal{F}^{(0)}, \mathcal{G}^{(0)}, t_1^{(0)}, t_2^{(0)}, w_1^{(0)} \dots w_5^{(0)}$.

If an autoparallel world line is assumed, using the parametrization of equations (23), it can be shown that the equation of motion to lowest order becomes

$$\frac{d\vec{v}}{dt} = - \left[t_1^{(0)} - \frac{\mathcal{H}^{(0)}}{2} \right] \frac{m_0}{r^2} \hat{e}_r. \quad (37)$$

Therefore Newton's Second Law interprets the mass of the central gravitating body to be

$$m = \left[t_1^{(0)} - \frac{\mathcal{H}^{(0)}}{2} \right] m_0. \quad (\text{autoparallel scheme}) \quad (38)$$

However, if $t_1^{(0)} - \mathcal{H}^{(0)}/2 = 0$, the autoparallel scheme fails totally.

Similarly, for a theory with extremal world-lines, the extremal equation in Newtonian approximation is

$$\frac{d\vec{v}}{dt} = - \frac{[-\mathcal{H}^{(0)}]}{2} \frac{m_0}{r^2} \hat{e}_r. \quad (39)$$

Therefore the physical mass of the body generating the gravity field is

$$m = -\frac{\mathcal{H}^{(0)}}{2} m_0, \quad (\text{extremal scheme}) \quad (40)$$

as long as $\mathcal{H}^{(0)} \neq 0$. For the Schwarzschild metric ($\mathcal{H}^{(0)} = -2$), $m = m_0$.

After re-scaling m from m_0 , all metric and torsion parameters make the inverse re-scaling, e.g. $t_1 = t_1^{(0)}(m_0/m)$ since the combination $t_1 m$ is the physical parameters during parametrization of metric and torsion. This inverse scaling applies to $\mathcal{H}^{(0)}, \mathcal{F}^{(0)}, \mathcal{G}^{(0)}, t_2^{(0)}, w_1^{(0)} \dots w_5^{(0)}$ as well. A natural consequence of the re-scaling is an identity by definition:

$$t_1 - \mathcal{H}/2 = 1, \quad (\text{autoparallel scheme}) \quad (41)$$

$$\text{or} \quad \mathcal{H} = -2, \quad (\text{extremal scheme}) \quad (42)$$

V. PRECESSION OF A GYROSCOPE II: INSTANTANEOUS RATE

We now have the tools to calculate the precession of a gyroscope. Before proceeding, let us summarize the assumptions made so far:

1. A gyroscope can feel torsion through its rotational angular momentum, and the equation of motion is either $DS^\mu/D\tau = 0$ or $DS^{\mu\nu}/D\tau = 0$.
2. The world line of a gyroscope is either an autoparallel curve or an extremal curve.
3. The torsion and connection around Earth are parametrized by Eq. (22) and (23).

With these assumptions, the calculation of the precession rate becomes straightforward except for one subtlety described below.

A. Transformation to the center-of-mass frame

The precession rate $d\vec{S}/dt$ derived from a naive application of the equation of motion $DS^\mu/D\tau = 0$ is the rate measured by an observer at rest relative to the central gravitating body. This rate is gauge-dependent and unphysical, since it depends on which coordinates the observer uses; for example, isotropic spherical coordinates and standard spherical coordinates yield different precession rates. The physical observable is the precession rate $d\vec{S}_0/dt$ measured by the observer co-moving with the center of mass of the gyroscope, i.e. in the instantaneous local inertial frame.

The methodology of transforming \vec{S} to \vec{S}_0 was first established by Schiff [76] in which he used the 4-tensor $S^{\mu\nu}$. The basic idea using the 4-vector S^μ is as follows. Since we are interested in the transformation only to leading order in $(v/c)^2$ and m/r , we are allowed to consider the coordinate transformation and the velocity transformation separately and add them together in the end. We adopt standard spherical coordinates with the line element of Eq. (21). The off-diagonal metric element proportional to ma/r^2 can be ignored for the purposes of

this transformation. Consider a measuring rod in the rest frame of the central body. It will be elongated by a factor of $(1 + \mathcal{F}m/2r)$ in the radial direction measured by the observer in the center-of-mass frame, but unchanged in the tangential direction. The 4-vector S^μ transforms as dx^μ ; thus its radial component is enlarged by a factor of $(1 + \mathcal{F}m/2r)$ and the tangential components are unchanged. This can be compactly written in the following form:

$$\vec{S}_0 = \vec{S} + \mathcal{F} \frac{m}{2r^3} (\vec{S} \cdot \vec{r}) \vec{r}. \quad (43)$$

Now consider the velocity transformation to the center-of-mass frame by boosting the observer along the x -axis, say, with velocity v . We have the Lorentz boost from $S^\mu = (S^0, S^x, S^y, S^z)$ to $S_0^\mu = (S_0^0, S_0^x, S_0^y, S_0^z)$ as follows:

$$S_0^0 = \gamma(S^0 - v S^x), \quad (44)$$

$$S_0^x = \gamma(S^x - v S^0), \quad (45)$$

$$S_0^y = S^y, \quad (46)$$

$$S_0^z = S^z, \quad (47)$$

where $\gamma = 1/\sqrt{1-v^2} \approx 1 + v^2/2$. The condition $S^\mu u_\mu = 0$ gives

$$S^0 = \vec{v} \cdot \vec{S} = v S^x,$$

which verifies that $S_0^0 = 0$ in the center-of-mass frame. The spatial components can be written compactly as

$$\vec{S}_0 = \vec{S} - \frac{1}{2} (\vec{S} \cdot \vec{v}) \vec{v}. \quad (48)$$

Combining the coordinate transformation and the velocity transformation, we find the following transformation from standard spherical coordinates to the center-of-mass frame:

$$\vec{S}_0 = \vec{S} + \mathcal{F} \frac{m}{2r^3} (\vec{S} \cdot \vec{r}) \vec{r} - \frac{1}{2} (\vec{S} \cdot \vec{v}) \vec{v}. \quad (49)$$

The time derivative of Eq. (49) will lead to the expression for *geodetic precession* to leading order, i.e. to order $(m/r)v$. To complete the discussion of transformations, note that the off-diagonal metric element proportional to ma/r^2 could add a term of order ma/r^2 to Eq. (49), which leads to a precession rate proportional to $(ma/r^2)v$. Since the leading term of the *frame dragging* effect is of the order ma/r^2 , the leading frame-dragging effect is invariant under these transformations, so we are allowed to ignore the off-diagonal metric element in the transformation.

The transformation law obtained using the 4-tensor $S^{\mu\nu}$ is different from using S^μ — this is not surprising because both descriptions coincide only in the rest frame of the gyroscope's center of mass. Schiff [76] gave the transformation law from standard spherical coordinates to the center-of-mass frame, using $S^{\mu\nu}$:

$$\begin{aligned} \vec{S}_0 &= \vec{S}' + \mathcal{F} \frac{m}{2r} [\vec{S}' - (\vec{r}/r^2)(\vec{r} \cdot \vec{S}')] \\ &\quad - \frac{1}{2} [v^2 \vec{S}' - (\vec{v} \cdot \vec{S}') \vec{v}]. \end{aligned} \quad (50)$$

In taking the time derivative of Eq. (49) or (50), one encounters terms proportional to $d\vec{v}/dt$. Eq. (37) or (39) should be applied, depending on whether autoparallel or extremal scheme, respectively, is assumed.

B. Instantaneous rates

1. Autoparallel scheme and using S^μ

Now we are now ready to calculate the precession rate. In spherical coordinates $x^\mu = (t, r, \theta, \phi)$, we expand the rotational angular momentum vector in an orthonormal basis:

$$\vec{S} = S_r \hat{e}_r + S_\theta \hat{e}_\theta + S_\phi \hat{e}_\phi.$$

In terms of the decomposition coefficients, the 4-vector is

$$S^\mu = (S^0, S^1, S^2, S^3) = (S^0, S_r, S_\theta/r, S_\phi/r \sin \theta).$$

Applying the equation of motion $DS^\mu/D\tau = 0$, transforming \vec{S} to \vec{S}_0 by Eq. (49) and taking the time derivative using autoparallels (Eq. 37), we obtain the following instantaneous gyroscope precession rate:

$$\frac{d\vec{S}_0}{dt} = \vec{\Omega} \times \vec{S}_0, \quad (51)$$

$$\text{where } \vec{\Omega} = \vec{\Omega}_G + \vec{\Omega}_F, \quad (52)$$

$$\vec{\Omega}_G = \left(\frac{\mathcal{F}}{2} - \frac{\mathcal{H}}{4} + t_2 + \frac{t_1}{2} \right) \frac{m}{r^3} (\vec{r} \times \vec{v}), \quad (53)$$

$$\begin{aligned} \vec{\Omega}_F &= \frac{\mathcal{G}I}{r^3} \left[-\frac{3}{2} (1 + \mu_1) (\vec{\omega}_E \cdot \hat{e}_r) \hat{e}_r \right. \\ &\quad \left. + \frac{1}{2} (1 + \mu_2) \vec{\omega}_E \right]. \end{aligned} \quad (54)$$

Here $I\omega_E = ma$ is the angular momentum of Earth, where I is Earth's moment of inertia about its poles and ω_E is its angular velocity. The new effective torsion constants are defined so that they represent the torsion-induced correction to the GR prediction:

$$\mu_1 \equiv (w_1 - w_2 - w_3 + 2w_4 + w_5)/(-3\mathcal{G}), \quad (55)$$

$$\mu_2 \equiv (w_1 - w_3 + w_5)/(-\mathcal{G}), \quad (56)$$

Since $t_1 - \mathcal{H}/2 = 1$ in the autoparallel scheme, Eq. (53) simplifies to

$$\vec{\Omega}_G = (1 + \mathcal{F} + 2t_2) \frac{m}{2r^3} (\vec{r} \times \vec{v}). \quad (57)$$

In the literature, the precession due to Ω_G is called *geodetic precession*, and that due to Ω_F is called *frame dragging*. From Eq. (53), it is seen that geodetic precession depends on the mass of Earth and not on whether Earth is spinning or not. It is of order mv . The frame-dragging effect is a unique effect of Earth's rotation and

highlights the importance of the GPB experiment, since GPB will be the first to accurately measure the effect of the off-diagonal metric element that lacks a counterpart in Newtonian gravity. The frame dragging effect is of order ma , so it is independent of whether the gyroscope is moving or static. In the presence of torsion, we term $\vec{\Omega}_G$ the “generalized geodetic precession”, and $\vec{\Omega}_F$ the “generalized frame-dragging”.

2. Extremal scheme and using S^μ

We now repeat the calculation of Section VB 1, but assuming an extremal trajectory (Eq. 39) when taking the time derivative of Eq. (49), obtaining the following instantaneous gyroscope precession rate:

$$\frac{d\vec{S}_0}{dt} = \vec{\Omega} \times \vec{S}_0 - t_1 \frac{m}{r^3} (\vec{S}_0 \cdot \vec{v}) \vec{r}, \quad (58)$$

$$\text{where } \vec{\Omega} = \vec{\Omega}_G + \vec{\Omega}_F.$$

$$\vec{\Omega}_G = \left(\frac{\mathcal{F}}{2} - \frac{\mathcal{H}}{4} + t_2 \right) \frac{m}{r^3} (\vec{r} \times \vec{v}), \quad (59)$$

and $\vec{\Omega}_F$ is the same as in Eq. (54). Since $\mathcal{H} = -2$ in the extremal scheme, Eq. (59) is simplified to formally coincide with Eq. (57).

3. Extremal scheme and using $S^{\mu\nu}$

In spherical coordinates, $S^{\mu\nu}$ satisfies

$$S^{12} = \frac{1}{r} S'_\phi, \quad S^{23} = \frac{1}{r^2 \sin \theta} S'_r, \quad S^{31} = \frac{1}{r \sin \theta} S'_\theta, \quad (60)$$

where S'_r, S'_θ, S'_ϕ are the components of \vec{S}' in spherical coordinates, i.e. $\vec{S}' = S'_r \hat{e}_r + S'_\theta \hat{e}_\theta + S'_\phi \hat{e}_\phi$. We now repeat the calculation of Section VB 1 assuming an extremal trajectory (Eq. 39) and the $S^{\mu\nu}$ -based precession of Eq. (50) when taking the time derivative of Eq. (49), obtaining the following instantaneous gyroscope precession rate:

$$\frac{d\vec{S}_0}{dt} = \vec{\Omega} \times \vec{S}_0 + t_1 \frac{m}{r^3} \vec{r} \times (\vec{v} \times \vec{S}_0), \quad (61)$$

$$\text{where } \vec{\Omega} = \vec{\Omega}_G + \vec{\Omega}_F.$$

$\vec{\Omega}_G$ and $\vec{\Omega}_F$ are the same as in equations (59) and (54), respectively.

In both cases using extremals, the precession rates have anomalous terms proportional to t_1 ; see Eq. (58) and (61). We call these terms the “anomalous geodetic precession”. These anomalies change the angular precession rate of a gyroscope, since their contributions to $d\vec{S}_0/dt$ are not perpendicular to \vec{S}_0 . This is a phenomenon that GR does not predict. Meanwhile, t_2 contributes to modify only the magnitude and not the direction of $\vec{\Omega}_G$. We therefore term t_1 the anomalous geodetic

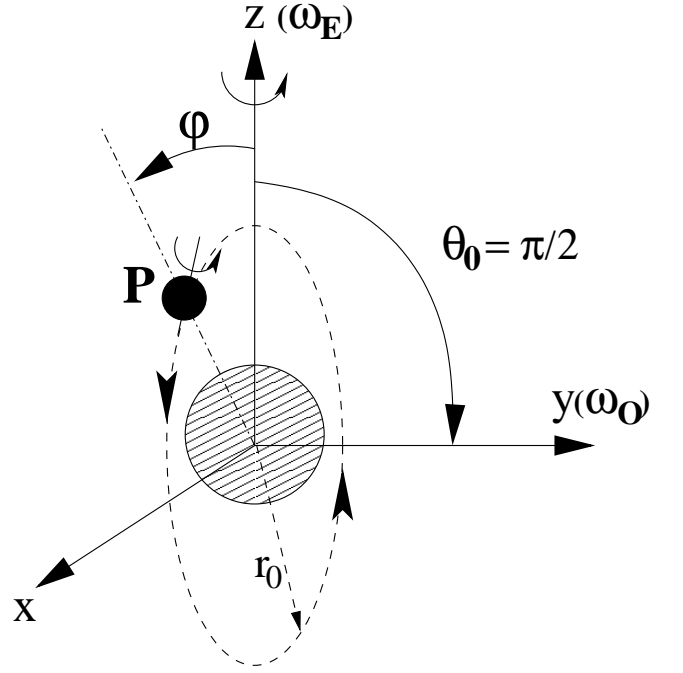


FIG. 2: A Gravity Probe B gyroscope moves around Earth along a circular polar orbit with $\theta_0 = \pi/2$. ω_O is its orbital angular velocity and ω_E is Earth’s rotational angular velocity around the z -axis.

torsion and t_2 the normal geodetic torsion. The torsion functions w_1, \dots, w_5 contribute to the generalized frame-dragging effect via the two combinations μ_1 and μ_2 , and we therefore term them “frame-dragging torsions”.

4. Autoparallel scheme and using $S^{\mu\nu}$

Repeating the calculation of Section VB 1 using the $S^{\mu\nu}$ -based precession rule of Eq. (50) gives the exact same instantaneous precession rate as in Section VB 1. This is expected since these two precession rules are equivalent in the autoparallel scheme.

VI. PRECESSION OF A GYROSCOPE III: MOMENT ANALYSIS

GPB measures the rotational angular momentum \vec{S}_0 of gyroscopes and therefore the precession rate $d\vec{S}_0/dt$ essentially continuously. This provides a wealth of information and deserves careful data analysis. Here we develop a simple but sensitive analysis method based on Fourier transforms.

A. Fourier transforms

The Gravity Probe B satellite has a circular polar orbit to good approximation⁷, i.e. the inclination angle of the orbital angular velocity $\vec{\omega}_O$ with respect to the Earth's rotation axis (z-axis) is $\theta_0 = \pi/2$. Hence the orbital plane is perpendicular to the equatorial plane. Let the y -axis point along the vector $\vec{\omega}_O$ and let the x -axis be perpendicular to the y -axis in the equatorial plane so that the three axes $\{x, y, z\}$ form a right-handed coordinate basis as illustrated in Figure 2. A gyroscope at a point P is marked by the monotonically increasing angle φ with respect to z axis. The polar angle of the point P can be regarded as a periodic function of φ :

$$\theta(\varphi) = \begin{cases} \varphi & , 0 \leq \varphi \leq \pi \\ 2\pi - \varphi & , \pi \leq \varphi \leq 2\pi \end{cases} \quad (62)$$

So for a particular circular polar orbit, $d\vec{S}_0/dt(\vec{r}, \vec{v})$ can be regarded as a periodic function of φ , where r_0 is the fixed radius, allowing us to write $d\vec{S}_0/dt(\vec{r}, \vec{v}) \equiv d\vec{S}_0/dt(\varphi)$.

Now define the Fourier *moments* of the precession rate as

$$\vec{a}_0 = \frac{1}{2\pi} \int_0^{2\pi} \frac{d\vec{S}_0}{dt}(\varphi) d\varphi = \left\langle \frac{d\vec{S}_0}{dt}(\varphi) \right\rangle, \quad (63)$$

$$\vec{a}_n = \frac{1}{2\pi} \int_0^{2\pi} \frac{d\vec{S}_0}{dt}(\varphi) \cos n\varphi d\varphi, \quad (64)$$

$$\vec{b}_n = \frac{1}{2\pi} \int_0^{2\pi} \frac{d\vec{S}_0}{dt}(\varphi) \sin n\varphi d\varphi, \quad (65)$$

where $n = 1, 2, \dots$, so that we can write

$$\frac{d\vec{S}_0}{dt}(\varphi) = \vec{a}_0 + 2 \sum_{n=1}^{\infty} (\vec{a}_n \cos n\varphi + \vec{b}_n \sin n\varphi). \quad (66)$$

B. Average precession

We now write equations (51), (52), (54), (57), (58) and (61) explicitly in terms of φ and perform the Fourier transforms. The average precession in the three calculation schemes above can be compactly written as follows:

$$\vec{a}_0 \equiv \left\langle \frac{d\vec{S}_0}{dt}(\varphi) \right\rangle = \vec{\Omega}_{\text{eff}} \times \vec{S}_0. \quad (67)$$

The angular precession rate is

$$\vec{\Omega}_{\text{eff}} = b_t \frac{3m}{2r_0} \vec{\omega}_O + b_\mu \frac{I}{2r_0^3} \vec{\omega}_E, \quad (68)$$

where $\vec{\omega}_O = \omega_O \hat{y}$ is the orbital angular velocity and $\vec{\omega}_E = \omega_E \hat{z}$ is the rotational angular velocity of Earth. Here the ‘‘biases’’ relative to the GR prediction are defined by

$$b_t \equiv \frac{1}{3}(1 + \mathcal{F} + 2t_2 + |\eta|t_1), \quad (69)$$

$$b_\mu \equiv \frac{(-\mathcal{G})}{2}(1 + 3\mu_1 - 2\mu_2), \quad (70)$$

$$= \frac{(-\mathcal{G})}{2}[1 + (w_1 + w_2 - w_3 - 2w_4 + w_5)/\mathcal{G}],$$

where the constant η reflects the different assumptions that we have explored, and takes the following values:

$$\eta = \begin{cases} 0 & \text{using autoparallels} \\ +1 & \text{using } S^{\mu\nu} \text{ and extremals} \\ -1 & \text{using } S^\mu \text{ and extremals} \end{cases} \quad (71)$$

From the above formulas, we see that the three schemes give identical results when $t_1 = 0$.

For comparison, GR predicts the average precession rate

$$\vec{a}_0 \equiv \left\langle \frac{d\vec{S}_0}{dt}(\varphi) \right\rangle = \vec{\Omega}_{\text{eff}} \times \vec{S}_0,$$

where $\vec{\Omega}_{\text{eff}} = \frac{3m}{2r_0} \vec{\omega}_O + \frac{I}{2r_0^3} \vec{\omega}_E,$ (72)

i.e. , $b_t = b_\mu = 1$.

It is important to note that torsion contributes to the *average* precession above only via *magnitudes* of the precession rates, leaving the precession axes intact. The geodetic torsion parameters t_1 and t_2 are degenerate, entering only in the linear combination corresponding to the bias b_t . The frame-dragging torsion parameters w_1, \dots, w_5 are similarly degenerate, entering only in the linear combination corresponding to the bias b_μ . If for technical reasons, the average precession rate is the only quantity that GPB can measure, then only these biases can be constrained.

C. Higher moments

Interestingly, all higher Fourier moments vanish except for $n = 2$:

$$\vec{a}_2 = \frac{-3\mathcal{G}I\omega_E}{8r_0^3}(1 + \mu_1)\hat{z} \times \vec{S}_0 + \eta t_1 \frac{m}{4r_0} \omega_O (S_0^x \hat{z} + S_0^z \hat{x}),$$

$$\vec{b}_2 = \frac{-3\mathcal{G}I\omega_E}{8r_0^3}(1 + \mu_1)\hat{x} \times \vec{S}_0 + \eta t_1 \frac{m}{4r_0} \omega_O (S_0^x \hat{x} - S_0^z \hat{z}). \quad (73)$$

⁷ The actual GPB orbit has an orbital eccentricity of 0.0014 and an inclination of 90.007° according to the Fact Sheet on the GPB website. These deviations from the ideal orbit should cause negligible ($\lesssim 10^{-5}$) relative errors in our estimates above.

Here we use the notation $S_0^i \equiv \vec{S}_0 \cdot \hat{i}$, where i denotes the x , y and z axes.

For comparison, GR predicts the following second moments (moments with $m = 1$ and $m > 2$ vanish):

$$\vec{a}_2 = \frac{3I\omega_E}{4r_0^3} \hat{z} \times \vec{S}_0, \quad (74)$$

$$\vec{b}_2 = \frac{3I\omega_E}{4r_0^3} \hat{x} \times \vec{S}_0. \quad (75)$$

Technically, it may be difficult to measure these second moments because of the extremely small precession rate per orbit. However, if they *could* be measured, they could break the degeneracy between t_1 and t_2 : $|t_1|$ could be measured through the *anomalous* $n = 2$ precession moment (the second term in Eq. (73)). The sign ambiguity of t_1 is due to the relative sign difference between the two schemes using extremals and $S^{\mu\nu}$ versus S^μ . The degeneracy between w_1, \dots, w_5 could be alleviated as well, since the linear combination μ_1 (defined in Eq. (55)) could be measured through the correction to the *normal* $n = 2$ precession moment (the first term in Eq. (73)). By “anomalous” or “normal”, we mean the term whose precession axis has not been or already been, respectively, predicted by GR. In addition, the anomalous second-moment terms cannot be expressed as the cross product of \vec{S}_0 and an angular velocity vector.

VII. CONSTRAINING TORSION PARAMETERS WITH GRAVITY PROBE B

The parametrized Post-Newtonian (PPN) formalism has over the past decades demonstrated its success as a theoretical framework of testing GR, by embedding GR in a broader parametrized class of metric theories of gravitation. This idea can be naturally generalized by introducing more general departures from GR, *e.g.* torsion. For solar system tests, the seven torsion parameters derived in Section III define the torsion extension of the PPN parameters, forming a complete set that parametrizes all observable signatures of torsion to lowest order.

However, most of existing solar system tests cannot constrain the torsion degrees of freedom. Photons are usually assumed to decouple from the torsion to preserve gauge invariance (we return below to the experimental basis of this), in which case tests using electromagnetic signals (*e.g.* Shapiro time delay and the deflection of light) can only constrain the metric, *i.e.* the PPN parameter γ , as we explicitly calculate in Appendix C 1 and Appendix C 2. Naively, one might expect that Mercury’s perihelion shift could constrain torsion parameters if Mercury’s orbit is an autoparallel curve, but calculations in Appendix C 4 and Appendix C 5 show that to lowest order, the perihelion shift is nonetheless only sensitive to the metric. Moreover, PPN calculations [3] show that a complete account of the perihelion

shift must involve second-order parameters in m/r (*e.g.* the PPN parameter β), which are beyond our first-order parametrization, as well as the first-order ones. We therefore neglect the constraining power of Mercury’s perihelion shift here. In contrast, the results in Section VIB show that Gravity Probe B will be very sensitive to torsion parameters even if only the average precession rates can be measured.

We may also constrain torsion with experimental upper bounds on the photon mass, since the “natural” extension of Maxwell Lagrangian ($\partial_\mu \rightarrow \nabla_\mu$ using the full connection) breaks gauge invariance and introduces anomalous electromagnetic forces and a quadratic term in A_μ that may be identified with the photon mass. In Appendix D, we estimate the constraints on the torsion parameters t_1 and t_2 from the measured photon mass limits, and show that these ground-based experiments can constrain t_1 or t_2 only to a level of the order unity, *i.e.*, not enough to be relevant to this paper.

In Appendix C, we confront solar system tests with the predictions from GR generalized with our torsion parameters. In general, it is natural to assume that all metric parameters take the same form as in PPN formalism⁸, *i.e.* [3]

$$\mathcal{H} = -2, \quad (76)$$

$$\mathcal{F} = 2\gamma, \quad (77)$$

$$\mathcal{G} = -(1 + \gamma + \frac{1}{4}\alpha_1). \quad (78)$$

Therefore, Shapiro time delay and the deflection of light share the same multiplicative bias factor $(\mathcal{F} - \mathcal{H})/4 = (1 + \gamma)/2$ relative to the GR prediction. The analogous bias for gravitational redshift is unity since $(\Delta\nu/\nu)/(\Delta\nu/\nu)^{(GR)} = -\mathcal{H}/2 = 1$. In contrast, both the geodetic precession and the frame-dragging effect have a non-trivial multiplicative bias in Eqs.(69) and (70):

$$b_t = \frac{1}{3}(1 + 2\gamma) + \frac{1}{3}(2t_2 + |\eta|t_1), \quad (79)$$

$$b_\mu = \frac{1}{2}(1 + \gamma + \frac{1}{4}\alpha_1) - \frac{1}{4}(w_1 + w_2 - w_3 - 2w_4 + w_5). \quad (80)$$

We list the observational constraints that solar system tests can place on the PPN and torsion parameters in Table II and plot the constraints in the degenerate parameter spaces in Figure 3. We see that GPB will ultimately constrain the linear combination $t_2 + \frac{|\eta|}{2}t_1$ (with η depending on the parallel transport scheme) at the 10^{-4} level and the combination $w_1 + w_2 - w_3 - 2w_4 + w_5$ at the 1% level. The unpublished preliminary results of GPB have confirmed the geodetic precession to less than 1%

⁸ This may not be completely true in some particular theories, *e.g.* $\mathcal{H} \neq -2$ in Einstein-Hayashi-Shirafuji theories in the autoparallel scheme, shown in Table IV.

level. This imposes a constraint on $|t_2 + \frac{|\eta|}{2}t_1| \lesssim 0.01$. The combination $w_1 + w_2 - w_3 - 2w_4 + w_5$ cannot be constrained by frame-dragging until GPB will manage to improve the accuracy to the target level of less than 1 milli-arcsecond.

VIII. LINEARIZED KERR SOLUTION WITH TORSION IN WEITZENBÖCK SPACETIME

So far, we have used only symmetry principles to derive the most general torsion possible around Earth to lowest order. We now turn to the separate question of whether there is any gravitational Lagrangian that actually produces torsion around Earth. We will show that the answer is yes by exploring the specific example of the Hayashi-Shirafuji Lagrangian [75] in Weitzenböck spacetime, showing that it populates a certain subset of the torsion degrees of freedom that we parametrized above and that this torsion mimics the Kerr metric to lowest order even though the Riemann curvature of spacetime vanishes. We begin with a brief review of Weitzenböck spacetime and the Hayashi-Shirafuji Lagrangian, then give the linearized solution in terms of the seven parameters $t_1, t_2, w_1, \dots, w_5$ from above. The solution we will derive is a particular special case of what the symmetry principles allow, and is for the particularly simple case where the Riemann curvature vanishes (Weitzenböck spacetime). Later in Section IX, we will give a more general Lagrangian producing both torsion and curvature, effectively interpolating between the Weitzenböck case below and standard GR.

We adopt the convention only here in Section VIII and Section IX that Latin letters are indices for the internal basis, whereas Greek letters are spacetime indices, both running from 0 to 3.

A. Weitzenböck spacetime

We give a compact review of Weitzenböck spacetime and Hayashi-Shirafuji Lagrangian here and in Section VIII B respectively. We refer the interested reader to their original papers [74, 75] for a complete survey of these subjects.

Weitzenböck spacetime is a Riemann-Cartan spacetime in which the Riemann curvature tensor, defined in Eq. (9), vanishes identically:

$$R^\rho{}_{\lambda\nu\mu}(\Gamma) = 0. \quad (81)$$

Figure 1 illustrates how Weitzenböck spacetime is related to other spacetimes.

Consider a local coordinate neighborhood of a point p in a Weitzenböck manifold with local coordinates x^μ . Introduce the coordinate basis $\{\bar{E}_\mu\} = \{(\partial/\partial x^\mu)_p\}$ and the dual basis $\{\bar{E}^\mu\} = \{(dx^\mu)_p\}$. A vector \bar{V} at p can be written as $\bar{V} = V^\mu \bar{E}_\mu$. The manifold is equipped with

an inner product; the metric is the inner product of the coordinate basis vectors,

$$g(\bar{E}_\mu, \bar{E}_\nu) = g(\bar{E}_\nu, \bar{E}_\mu) = g_{\mu\nu}.$$

There exists a quadruplet of orthonormal vector fields $\bar{e}_k(p)$, where $\bar{e}_k(p) = e_k^\mu(p)\bar{E}_\mu$, such that

$$g(\bar{e}_k, \bar{e}_l) = g_{\mu\nu}e_k^\mu e_l^\nu = \eta_{kl}, \quad (82)$$

where $\eta_{kl} = \text{diag}(-1, 1, 1, 1)$. There also exists a dual quadruplet of orthonormal vector fields $\bar{e}^k(p)$, where $\bar{e}^k(p) = e^k_\mu(p)\bar{E}^\mu$, such that

$$e_k^\mu e^\nu{}_\mu = \delta^\mu{}_\nu, \quad e_k^\mu e^l{}_\mu = \delta_k^l. \quad (83)$$

This implies that

$$\eta_{kl}e^k{}_\mu e^l{}_\nu = g_{\mu\nu}. \quad (84)$$

which is often phrased as the 4×4 matrix \mathbf{e} (a.k.a. the *tetrad* or *vierbein*) being “the square root of the metric”.

An alternative definition of Weitzenböck spacetime that is equivalent to that of Eq. (81) is the requirement that the Riemann-Cartan spacetime admit a quadruplet of linearly independent *parallel vector fields* e_k^μ , defined by⁹

$$\nabla_\mu e_k^\nu = \partial_\mu e_k^\nu + \Gamma^\nu{}_{\mu\lambda} e_k^\lambda = 0. \quad (85)$$

Solving this equation, one finds that

$$\Gamma^\lambda{}_{\mu\nu} = e_k^\lambda \partial_\mu e^\nu{}_\nu, \quad (86)$$

and that the torsion tensor

$$S_{\mu\nu}{}^\lambda = \frac{1}{2}e_k^\lambda (\partial_\mu e^\nu{}_\nu - \partial_\nu e^\mu{}_\mu). \quad (87)$$

This property of allowing globally parallel basis vector fields was termed “teleparallelism” by Einstein, since it allows unambiguous parallel transport, and formed the foundation of the torsion theory he termed “new general relativity” [88–103].

A few additional comments are in order:

1. It is easy to verify that the first definition of Weitzenböck spacetime (as curvature-free, i.e. via Eq. (81)) follows from the second definition — one simply uses the the explicit expression for the connection (Eq. 86). It is also straightforward to verify that $\nabla_\mu g_{\nu\rho} = 0$ using Eq. (84) and (85).
2. Eq. (86) is form invariant under general (spacetime) coordinate transformations due to the non-linear transformation law (Eq. (18)) of the connection, provided that e_k^μ and e^k_μ transform as a contravariant vector and a covariant vector, respectively.

⁹ Note that Hayashi and Shirafuji [75] adopted a convention where the order of the lower index placement in the connection is opposite to that in Eq. (85).

Effects	Torsion Biases	Observ. Constraints	Remarks
Shapiro time delay	$\Delta t/\Delta t^{(GR)} = (1 + \gamma)/2$	$\gamma - 1 = (2.1 \pm 2.3) \times 10^{-5}$	Cassini tracking [122]
Deflection of light	$\delta/\delta^{(GR)} = (1 + \gamma)/2$	$\gamma - 1 = (-1.7 \pm 4.5) \times 10^{-4}$	VLBI [123]
Gravitational redshift	$(\Delta\nu/\nu)/(\Delta\nu/\nu)^{(GR)} = 1$	no constraints	
Geodetic Precession	$\Omega_G/\Omega_G^{(GR)} = b_t$	$(\gamma - 1) + (t_2 + \frac{ \eta }{2}t_1) < 1.1 \times 10^{-4}$	Gravity Probe B
Frame-dragging	$\Omega_F/\Omega_F^{(GR)} = b_\mu$	$ (\gamma - 1 + \frac{1}{4}\alpha_1) - \frac{1}{2}(w_1 + w_2 - w_3 - 2w_4 + w_5) < 0.024$	Gravity Probe B

TABLE II: Constraints of PPN and torsion parameters with solar system tests. The observational constraints on PPN parameters are taken from Table 4 of [3]. Unpublished preliminary results of Gravity Probe B have confirmed geodetic precession to better than 1%, giving a constraint $|(\gamma - 1) + (t_2 + \frac{|\eta|}{2}t_1)| \lesssim 0.01$. The full GPB results are yet to be released, so whether the frame dragging will agree with the GR prediction is not currently known. The last two rows show the limits that would correspond to a GPB result consistent with GR, assuming an angle accuracy of 0.5 milli-arcseconds.

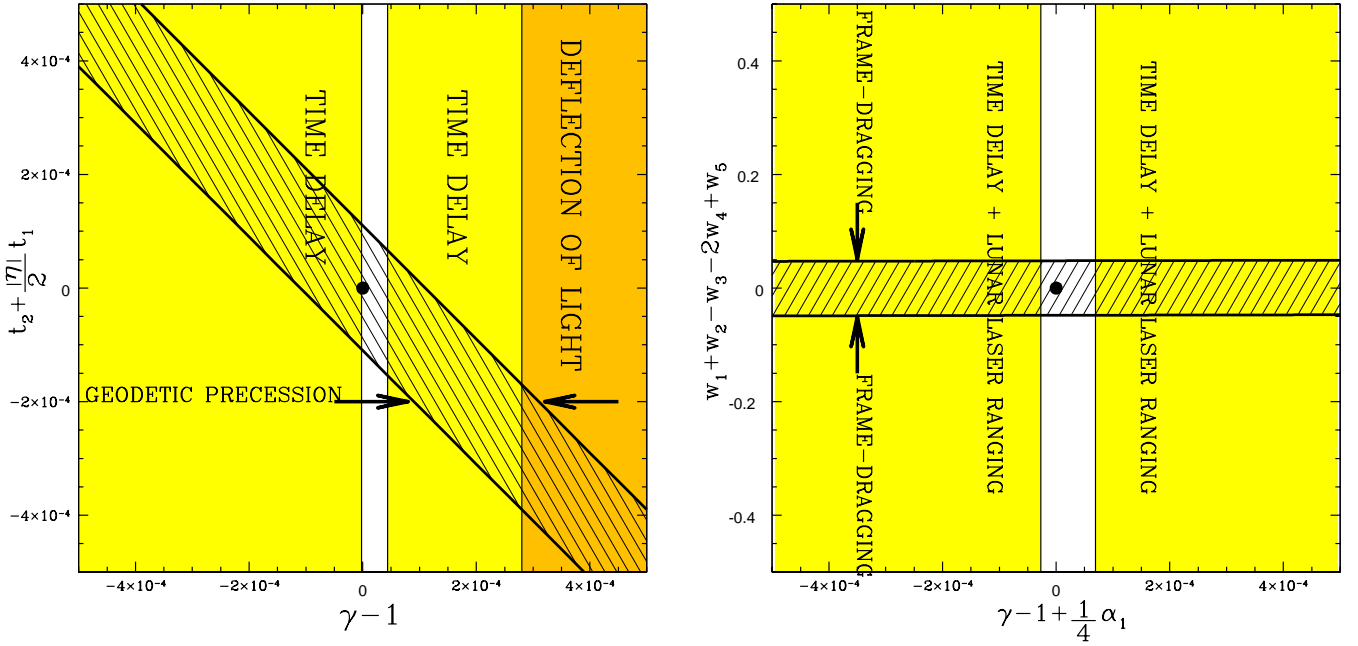


FIG. 3: constraints on the PPN parameters (γ , α_1) and torsion parameters (t_1 , t_2 , $w_1 \dots w_5$) from solar system tests. General Relativity corresponds to the black dot ($\gamma - 1 = \alpha_1 =$ all torsion parameters = 0). Left panel: the shaded regions in the parameter space have already been ruled out by the deflection of light (orange/grey) and Shapiro time delay (yellow/light grey). Gyroscope experiments are sensitive to torsion parameters. If the geodetic precession measured by Gravity Probe B is consistent with GR, this will rule out everything outside the hatched region, implying that $-1.5 \times 10^{-4} < t_2 + \frac{|\eta|}{2}t_1 < 1.1 \times 10^{-4}$ (assuming a target angle accuracy of 0.5 milli-arcseconds). The unpublished preliminary results of Gravity Probe B have confirmed the geodetic precession to better than 1%, giving a constraint $|t_2 + \frac{|\eta|}{2}t_1| \lesssim 0.01$. Right panel: the shaded regions in the parameter space have already been ruled out by Shapiro time delay combined with lunar laser ranging experiment (yellow/light grey). Lunar laser ranging constrains $|\alpha_1| < 10^{-4}$ [3]. If the frame-dragging effect measured by Gravity Probe B is consistent with GR, this will rule out everything outside the hatched region, implying that $|w_1 + w_2 - w_3 - 2w_4 + w_5| < 4.8 \times 10^{-2}$.

3. The Weitzenböck spacetime preserves its geometry under *global* proper orthochronous Lorentz transformations, i.e. a new equivalent quadruplet of parallel vector fields \underline{e}' is obtained by a global proper orthochronous Lorentz transformation, $e'^{\mu}_k = \Lambda^{\mu}_k e_l^{\mu}$.

B. Hayashi-Shirafuji Lagrangian

The Hayashi-Shirafuji Lagrangian [75] is a gravitational Lagrangian density constructed in the geometry

of Weitzenböck spacetime¹⁰. It is a Poincaré gauge theory in that the parallel vector fields \underline{e}_k (rather than the metric or torsion) are the basic entities with respect to which the action is varied to obtain the gravitational field equations.

First, note that the torsion tensor in Eq. (87) is *reducible* under the group of global Lorentz transformation. It can be decomposed into three irreducible parts under this Lorentz group [119]¹¹, i.e. into parts which do not mix under a global Lorentz transformation:

$$t_{\lambda\mu\nu} = \frac{1}{2}(S_{\nu\mu\lambda} + S_{\nu\lambda\mu}) + \frac{1}{6}(g_{\nu\lambda}v_\mu + g_{\nu\mu}v_\lambda) - \frac{1}{3}g_{\lambda\mu}v_\nu, \quad (88)$$

$$v_\mu = S_{\mu\lambda}{}^\lambda, \quad (89)$$

$$a_\mu = \frac{1}{6}\bar{\epsilon}_{\mu\nu\rho\sigma}S^{\sigma\rho\nu}, \quad (90)$$

Here $\bar{\epsilon}_{\mu\nu\rho\sigma} = \sqrt{-g}\epsilon_{\mu\nu\rho\sigma}$ and $\bar{\epsilon}^{\mu\nu\rho\sigma} = \epsilon^{\mu\nu\rho\sigma}/\sqrt{-g}$ are 4-tensors, and the Levi-Civita symbol is normalized such that $\epsilon_{0123} = -1$ and $\epsilon^{0123} = +1$. The tensor $t_{\lambda\mu\nu}$ satisfies $t_{\lambda\mu\nu} = t_{\mu\lambda\nu}$, $g^{\mu\nu}t_{\lambda\mu\nu} = g^{\lambda\mu}t_{\lambda\mu\nu} = 0$, and $t_{\lambda\mu\nu} + t_{\mu\nu\lambda} + t_{\nu\lambda\mu} = 0$. Conversely, the torsion can be written in terms of its irreducible parts as

$$S_{\nu\mu\lambda} = \frac{2}{3}(t_{\lambda\mu\nu} - t_{\lambda\nu\mu}) + \frac{1}{3}(g_{\lambda\mu}v_\nu - g_{\lambda\nu}v_\mu) + \bar{\epsilon}_{\lambda\mu\nu\rho}a^\rho. \quad (91)$$

In order that the field equation be a second-order differential equation in \underline{e}_k (so that torsion can propagate), the Lagrangian is required to be quadratic in the torsion tensor. In addition, the Lagrangian should be invariant under the group of general coordinate transformations, under the global proper orthochronous Lorentz group, and under parity reversal in the internal basis ($\underline{e}_0 \rightarrow \underline{e}_0$, $\underline{e}_a \rightarrow -\underline{e}_a$). Hayashi and Shirafuji suggested the gravitational action of the following form [75]:

$$I_G = \int d^4x \sqrt{-g} \left[\frac{1}{2\kappa} R(\{\}) + c_1 t^{\lambda\mu\nu} t_{\lambda\mu\nu} + c_2 v^\mu v_\mu + c_3 a^\mu a_\mu \right], \quad (92)$$

where c_1, c_2, c_3 are three free parameters, $R(\{\})$ is the scalar curvature calculated using the Levi-Civita connection and $\kappa = 8\pi G/c^4$. The *vacuum* field equations are obtained by varying this action with respect to the tetrad $e^k{}_\nu$ and then multiplying by $\eta^{kj}e_j{}^\mu$. Note that in Hayashi-Shirafuji theory, the torsion (or equivalently,

the connection) is not an independent variable as in some standard torsion theories [42]. Instead, the torsion is exclusively determined by the tetrad via Eq. (87). The resultant field equation is

$$\frac{1}{2\kappa} G^{\mu\nu}(\{\}) + \nabla_\lambda F^{\mu\nu\lambda} + v_\lambda F^{\mu\nu\lambda} + H^{\mu\nu} - \frac{1}{2}g^{\mu\nu}L_2 = 0. \quad (93)$$

Here the first term denotes the Einstein tensor calculated using the Levi-Civita connection, but the field equation receives important non-Riemannian contributions from torsion through the other terms. The other tensors in Eq. (93) are defined as follows:

$$F^{\mu\nu\lambda} = c_1(t^{\mu\nu\lambda} - t^{\mu\lambda\nu}) + c_2(g^{\mu\nu}v^\lambda - g^{\mu\lambda}v^\nu) - \frac{1}{3}c_3\bar{\epsilon}^{\mu\nu\lambda\rho}a_\rho, \quad (94)$$

$$H^{\mu\nu} = 2S^{\mu\sigma\rho}F_{\rho\sigma}{}^\nu - S^{\sigma\rho\nu}F_{\rho\sigma}{}^\mu, \quad (95)$$

$$L_2 = c_1 t^{\lambda\mu\nu} t_{\lambda\mu\nu} + c_2 v^\mu v_\mu + c_3 a^\mu a_\mu. \quad (96)$$

Since torsion is the first derivative of the tetrad as per Eq. (87), the field equation is a nonlinear second-order differential equation of the tetrad. Consequently, the tetrad (hence the torsion) can propagate in the vacuum.

C. Static, spherically and parity symmetric vacuum solution

Hayashi and Shirafuji derived the exact static, spherically and parity symmetric $R_{\mu\nu\rho\sigma} = 0$ vacuum solutions for this Lagrangian in [75]. The parallel vector fields take the following form in isotropic rectangular coordinates (here Latin letters are spatial indices) [75]:

$$\begin{aligned} e_0^0 &= \left(1 - \frac{m_0}{pr}\right)^{-p/2} \left(1 + \frac{m_0}{qr}\right)^{q/2}, \\ e_0^i &= e_a^i = 0, \\ e_a^i &= \left(1 - \frac{m_0}{pr}\right)^{-1+p/2} \left(1 + \frac{m_0}{qr}\right)^{-1-q/2} \delta_a^i, \end{aligned} \quad (97)$$

where m_0 is a parameter with units of mass and will be related to the physical mass of the central gravitating body in Section X. The new parameters p and q are functions of a dimensionless parameter ϵ :

$$\epsilon \equiv \frac{\kappa(c_1 + c_2)}{1 + \kappa(c_1 + 4c_2)}, \quad (98)$$

$$p \equiv \frac{2}{1 - 5\epsilon} \{[(1 - \epsilon)(1 - 4\epsilon)]^{1/2} - 2\epsilon\}, \quad (99)$$

$$q \equiv \frac{2}{1 - 5\epsilon} \{[(1 - \epsilon)(1 - 4\epsilon)]^{1/2} + 2\epsilon\}. \quad (100)$$

Here $\kappa = 8\pi G$.

The line element in the static, spherically and parity

¹⁰ The Hayashi-Shirafuji theory differs from the teleparallel gravity theory described in [104, 105], which is argued to be fully equivalent to GR.

¹¹ Note that we denote the irreducible parts (i.e. $t_{\lambda\mu\nu}, v_\mu, a_\mu$) by the same letters as in [75], but that these quantities here are only one half as large as in [75], due to different conventions in the definition of torsion. Similarly, the quantities c_1, c_2, c_3 in Eq. (92) are four times as large as in [75].

symmetric field takes the exact form [75]

$$ds^2 = - \left(1 - \frac{m_0}{pr}\right)^p \left(1 + \frac{m_0}{qr}\right)^{-q} dt^2 + \left(1 - \frac{m_0}{pr}\right)^{2-p} \left(1 + \frac{m_0}{qr}\right)^{2+q} dx^i dx^i \quad (101)$$

In order to generalize this solution to the axisymmetric case, we transform the parallel vector fields into standard spherical coordinates and keep terms to first order in m_0/r (the subscript “sp” stands for “spherical”):

$$e_{(\text{sp})k}{}^\mu = \downarrow_k \begin{pmatrix} \rightarrow \mu \\ 1 + \frac{m_0}{r} & 0 & 0 & 0 \\ 0 & \left[1 - \frac{m_0}{r} \left(1 + \frac{1}{q} - \frac{1}{p}\right)\right] \sin \theta \cos \phi & \frac{\cos \theta \cos \phi}{r} & -\frac{\csc \theta \sin \phi}{r} \\ 0 & \left[1 - \frac{m_0}{r} \left(1 + \frac{1}{q} - \frac{1}{p}\right)\right] \sin \theta \sin \phi & \frac{\cos \theta \sin \phi}{r} & \frac{\csc \theta \cos \phi}{r} \\ 0 & \left[1 - \frac{m_0}{r} \left(1 + \frac{1}{q} - \frac{1}{p}\right)\right] \cos \theta & -\frac{\sin \theta}{r} & 0 \end{pmatrix} \quad (102)$$

A particularly interesting solution is that for the parameter choice $c_1 = -c_2$ so that $\epsilon = 0$ and $p = q = 2$. Eq. (101) shows that the resultant metric coincides with the Schwarzschild metric around an object of mass m_0 . The parameter c_3 is irrelevant here because of the static, spherically and parity symmetric field. When $c_1 + c_2$ is small but nonzero, we have $\epsilon \ll 1$ and

$$p = 2 + \epsilon + \mathcal{O}(\epsilon^2), \quad (103)$$

$$q = 2 + 9\epsilon + \mathcal{O}(\epsilon^2). \quad (104)$$

By using equations (84), (86) and (87), we find that the linearized metric and torsion match our parametrization in Section III A. When $\epsilon \ll 1$, the line element is

$$ds^2 = - \left[1 - 2\frac{m_0}{r}\right] dt^2 + \left[1 + 2(1 - 2\epsilon)\frac{m_0}{r}\right] dr^2 + r^2 d\Omega^2, \quad (105)$$

and the torsion is

$$S_{tr}{}^t = -\frac{m_0}{2r^2}, \quad (106)$$

$$S_{r\theta}{}^\theta = S_{r\phi}{}^\phi = -(1 - 2\epsilon)\frac{m_0}{2r^2}, \quad (107)$$

both to linear order in m_0/r .

D. Solution around Earth

We now investigate the field generated by a uniformly rotating spherical body to first order in ϵ_a . It seems reasonable to assume that to first order the metric coincides with the Kerr-like metric, i.e.

$$g_{t\phi} = \mathcal{G}_0(m_0 a/r) \sin^2 \theta, \quad (108)$$

around an object of specific angular momentum a in the linear regime $m_0/r \ll 1$ and $a/r \ll 1$. Since the Kerr-like

metric automatically satisfies $G(\{ \}) = 0$ in vacuum, the vacuum field equation reduces to

$$\nabla_\lambda F^{\mu\nu\lambda} + v_\lambda F^{\mu\nu\lambda} + H^{\mu\nu} - \frac{1}{2}g^{\mu\nu}L_2 = 0. \quad (109)$$

We now employ our parametrization with “mass” in Eq. (22) replaced by m_0 , where m_0 is the parameter in accordance with Section VIII C. In Section X, we will apply the Kerr solution $\mathcal{G} = -2$ after re-scaling m_0 to correspond to the physical mass. Imposing the no-curvature condition $R_{\mu\nu\rho\sigma} = 0$, we find that this condition and Eq. (109) are satisfied to lowest order in m_0/r and a/r if

$$\begin{aligned} w_1^{(0)} &= \mathcal{G}_0 - \alpha_0, \\ w_2^{(0)} &= -2(\mathcal{G}_0 - \alpha_0), \\ w_3^{(0)} &= w_4^{(0)} = \alpha_0, \\ w_5^{(0)} &= 2\alpha_0. \end{aligned} \quad (110)$$

Here a superscript (0) indicates the parametrization with m_0 in place of m . α_0 is an undetermined constant and should depend on the Lagrangian parameters c_1 , c_2 and c_3 . This parameter has no effect on the precession of a gyroscope or on any of the other observational constraints that we consider, so its value is irrelevant to the present paper.

The parallel vector fields that give the Kerr metric, the connection and the torsion (including the spherically symmetric part) via equations (83)–(84) and (86)–(87) take the following form to linear order:

$$e_k{}^\mu = e_{(\text{sp})k}{}^\mu + \downarrow_k \begin{pmatrix} \rightarrow \mu \\ 0 & 0 & 0 & -\alpha_0 \frac{m_0 a}{r^3} \\ -(\mathcal{G}_0 - \alpha_0) \frac{m_0 a \sin \theta \sin \phi}{r^2} & 0 & 0 & 0 \\ (\mathcal{G}_0 - \alpha_0) \frac{m_0 a \sin \theta \cos \phi}{r^2} & 0 & 0 & 0 \\ 0 & 0 & 0 & 0 \end{pmatrix} \quad (111)$$

IX. A TOY MODEL: LINEAR INTERPOLATION IN RIEMANN-CARTAN SPACE BETWEEN GR AND HAYASHI-SHIRAFUJI LAGRANGIAN

We found that the Hayashi-Shirafuji Lagrangian admits both the Schwarzschild metric and (at least to linear order) the Kerr metric, but in the Weitzenböck spacetime where there is no Riemann curvature and all spacetime structure is due to torsion. This is therefore an opposite extreme of GR, which admits these same metrics in Riemann spacetime with all curvature and no torsion. Both of these solutions can be embedded in Riemann-Cartan spacetime, and we will now present a more general two-parameter family of Lagrangians that interpolates between these two extremes, always allowing the Kerr metric and generally explaining the spacetime distortion with a combination of curvature and torsion. After the first version of this paper was submitted, Flanagan and Rosenthal showed that the Einstein-Hayashi-Shirafuji Lagrangian has serious defects [126], while leaving open the possibility that there may be other viable Lagrangians in the same class (where spinning objects generate and feel propagating torsion). This Lagrangian should therefore not be viewed as a viable physical model, but as a pedagogical toy model admitting both curvature and torsion, giving concrete illustrations of the various effects and constraints that we discuss.

This family of theories, which we will term Einstein-Hayashi-Shirafuji (EHS) theories, have an action in Riemann-Cartan space of the form

$$I_G = \int d^4x \sqrt{-g} \left[\frac{1}{2\kappa} R(\{\}) + \sigma^2 c_1 t^{\lambda\mu\nu} t_{\lambda\mu\nu} + \sigma^2 c_2 v^\mu v_\mu + \sigma^2 c_3 a^\mu a_\mu \right] \quad (112)$$

where σ is a parameter in the range $0 \leq \sigma \leq 1$. Here the tensors $t_{\lambda\mu\nu}$, v_μ and a_μ are the decomposition (in accordance with Eqs.88–90) of $\sigma^{-1} S_{\nu\mu\lambda}$, which is independent of σ and depends only on $e^i{}_\mu$ as per Eq. (114). The function σ^2 associated with the coefficients c_1 , c_2 and c_3 in Eq. (112) may be replaced by any other regular function of σ that approaches to zero as $\sigma \rightarrow 0$. The metric in the EHS theories is defined in Eq. (84). Similar to the Hayashi-Shirafuji theory, the field equation for EHS theories is obtained by varying the action with respect to the tetrad. The resultant field equation is identical to that for the Hayashi-Shirafuji Lagrangian (Eq. 93) except for the replacement $c_{1,2,3} \rightarrow \sigma^2 c_{1,2,3}$. Also, the $S^{\mu\sigma\rho}$ in Eq. (95) is replaced by $\sigma^{-1} S^{\mu\sigma\rho}$. Thus the EHS Lagrangian admits the same solution for $e_k{}^\mu$. Since the metric is independent of the parameter σ , the EHS Lagrangian admits both the spherically symmetric metric in Eq. (101) and the Kerr-like metric in Eq. (108), at least to the linear order. For the spherically symmetric metric, the parameter ϵ in Hayashi-Shirafuji theory is generalized to a new parameter τ in EHS theories, de-

fining by the replacement $c_{1,2} \rightarrow \sigma^2 c_{1,2}$:

$$\tau \equiv \frac{\kappa\sigma^2(c_1 + c_2)}{1 + \kappa\sigma^2(c_1 + 4c_2)}. \quad (113)$$

The torsion around Earth is linearly proportional to σ , given by the parameter σ times the solution in Eq. (106) and (110):

$$S_{\mu\nu}{}^\lambda \equiv \frac{\sigma}{2} e_k{}^\lambda (\partial_\mu e^k{}_\nu - \partial_\nu e^k{}_\mu). \quad (114)$$

By virtue of Eq. (7) (the metric compatibility condition), it is straightforward to show that the connection is of the form

$$\Gamma^\rho{}_{\mu\nu} = (1 - \sigma) \left\{ \begin{matrix} \rho \\ \mu\nu \end{matrix} \right\} + \sigma e_k{}^\rho \partial_\mu e^k{}_\nu. \quad (115)$$

EHS theory thus interpolates smoothly between metric gravity *e.g.* GR ($\sigma = 0$) and the all-torsion Hayashi-Shirafuji theory ($\sigma = 1$). If $\sigma \neq 1$, it is straightforward to verify that the curvature calculated by the full connection does not vanish. Therefore, the EHS theories live in neither Weitzenböck space nor the Riemann space, but in the Riemann-Cartan space that admits both torsion and curvature.

It is interesting to note that since the Lagrangian parameters c_1 and c_2 are independent of the torsion parameter σ , the effective parameter τ is not necessarily equal to zero when $\sigma = 0$ (i.e. , $\sigma^2 c_1$ or $\sigma^2 c_2$ can be still finite). In this case ($\sigma = 0$ and yet $\tau \neq 0$), obviously this EHS theory is an extension to GR without adding torsion. In addition to the extra terms in the Lagrangian of Eq. (112), the extension is subtle in the symmetry of the Lagrangian. In the tetrad formalism of GR, *local* Lorentz transformations are symmetries in the internal space of tetrads. Here in this $\sigma = 0, \tau \neq 0$ EHS theory, the allowed internal symmetry is *global* Lorentz transformations as in the Weitzenböck spacetime, because $t_{\lambda\mu\nu}$, v_μ and a_μ contain the partial derivatives of tetrads (see Eq. 114). So the $\sigma = 0$ and $\tau \neq 0$ EHS theory is a tetrad theory in Riemann spacetime with less gauge freedom.

Since GR is so far consistent with all known observations, it is interesting to explore (as we will below) what observational upper limits can be placed on both σ and τ .

X. EXAMPLE: TESTING EINSTEIN HAYASHI-SHIRAFUJI THEORIES WITH GPB AND OTHER SOLAR SYSTEM EXPERIMENTS

Above we calculated the observable effects that arbitrary Earth-induced torsion, if present, would have on GPB. As a foil against which to test GR, let us now investigate the observable effects that would result for the explicit Einstein-Hayashi-Shirafuji class of torsion theories that we studied in Section VIII D and IX.

		Hayashi-Shirafuji with m_0	EHS with m_0	Definitions
metric parameters	$\mathcal{H}^{(0)}$	-2	-2	$g_{tt} = -1 - \mathcal{H}^{(0)} m_0/r + \mathcal{O}(m_0/r)^2$
	$\mathcal{F}^{(0)}$	$2(1 - 2\epsilon)$	$2(1 - 2\tau)$	$g_{rr} = 1 + \mathcal{F}^{(0)} m_0/r + \mathcal{O}(m_0/r)^2$
geodetic torsions	$t_1^{(0)}$	-1	$-\sigma$	anomalous, $S_{tr}{}^t = t_1^{(0)} m_0/2r^2$
	$t_2^{(0)}$	$-(1 - 2\epsilon)$	$-\sigma(1 - 2\tau)$	normal, $S_{r\theta}{}^\theta = S_{r\phi}{}^\phi = t_2^{(0)} m_0/2r^2$
frame-dragging torsions	$w_1^{(0)}$	$\mathcal{G}_0 - \alpha_0$	$\sigma(\mathcal{G}_0 - \alpha_0)$	$S_{r\phi}{}^t = w_1^{(0)} (m_0 a/2r^2) \sin^2 \theta$
	$w_2^{(0)}$	$-2(\mathcal{G}_0 - \alpha_0)$	$-2\sigma(\mathcal{G}_0 - \alpha_0)$	$S_{\theta\phi}{}^t = w_2^{(0)} (m_0 a/2r) \sin \theta \cos \theta$
	$w_3^{(0)}$	α_0	$\sigma\alpha_0$	$S_{t\phi}{}^r = w_3^{(0)} (m_0 a/2r^2) \sin^2 \theta$
	$w_4^{(0)}$	α_0	$\sigma\alpha_0$	$S_{t\phi}{}^\theta = w_4^{(0)} (m_0 a/2r^3) \sin \theta \cos \theta$
	$w_5^{(0)}$	$2\alpha_0$	$2\sigma\alpha_0$	$S_{tr}{}^\phi = w_5^{(0)} m_0 a/2r^4$

TABLE III: Summary of metric and torsion parameters for General Relativity, Hayashi-Shirafuji gravity and Einstein-Hayashi-Shirafuji (EHS) theories. The subscript 0 indicates all parameter values are normalized by an arbitrary constant m_0 (with the units of mass) that is not necessarily the physical mass of the body generating the gravity. The parameter α_0 in frame-dragging torsions is an undetermined constant and should depend on the Hayashi-Shirafuji Lagrangian parameters c_1 , c_2 and c_3 . The parameter τ , defined in Eq. (98) and assumed small, is an indicator of how close the emergent metric is to the Schwarzschild metric. The values in the column of Einstein-Hayashi-Shirafuji interpolation are those in the Hayashi-Shirafuji *times* the interpolation parameter σ .

		GR	EHS with autoparallels	EHS with extremals	Definitions
mass	m	$m = m_0$	$m = (1 - \sigma)m_0$	$m = m_0$	set by Newtonian limit
metric parameters	\mathcal{H}	-2	$-2/(1 - \sigma)$	-2	$g_{tt} = -1 - \mathcal{H}m/r + \mathcal{O}(m/r)^2$
	\mathcal{F}	2	$2(1 - 2\tau)/(1 - \sigma)$	$2(1 - 2\tau)$	$g_{rr} = 1 + \mathcal{F}m/r + \mathcal{O}(m/r)^2$
	\mathcal{G}	-2	-2	-2	$g_{t\phi} = \mathcal{G}(ma/r) \sin^2 \theta$
geodetic torsions	t_1	0	$-\sigma/(1 - \sigma)$	$-\sigma$	anomalous, $S_{tr}{}^t = t_1 m/2r^2$
	t_2	0	$-\sigma(1 - 2\tau)/(1 - \sigma)$	$-\sigma(1 - 2\tau)$	normal, $S_{r\theta}{}^\theta = S_{r\phi}{}^\phi = t_2 m/2r^2$
frame-dragging torsions	w_1	0	$\sigma(\mathcal{G} - \alpha)$	$\sigma(\mathcal{G} - \alpha)$	$S_{r\phi}{}^t = w_1 (ma/2r^2) \sin^2 \theta$
	w_2	0	$-2\sigma(\mathcal{G} - \alpha)$	$-2\sigma(\mathcal{G} - \alpha)$	$S_{\theta\phi}{}^t = w_2 (ma/2r) \sin \theta \cos \theta$
	w_3	0	$\sigma\alpha$	$\sigma\alpha$	$S_{t\phi}{}^r = w_3 (ma/2r^2) \sin^2 \theta$
	w_4	0	$\sigma\alpha$	$\sigma\alpha$	$S_{t\phi}{}^\theta = w_4 (ma/2r^3) \sin \theta \cos \theta$
	w_5	0	$2\sigma\alpha$	$2\sigma\alpha$	$S_{tr}{}^\phi = w_5 ma/2r^4$
effective torsions	μ_1	0	$-\sigma$	$-\sigma$	$\mu_1 = (w_1 - w_2 - w_3 + 2w_4 + w_5)/(-3\mathcal{G})$
	μ_2	0	$-\sigma$	$-\sigma$	$\mu_2 = (w_1 - w_3 + w_5)/(-\mathcal{G})$
bias	b_t	1	$1 - 4\tau/3$	$1 - \sigma - 4\tau/3$	$b_t = (1 + \mathcal{F} + 2t_2 + \eta t_1)/3$
	b_μ	1	$(-\mathcal{G}/2)(1 - \sigma)$	$(-\mathcal{G}/2)(1 - \sigma)$	$b_\mu = (-\mathcal{G}/2)(1 + 3\mu_1 - 2\mu_2)$

TABLE IV: Summary of metric and torsion parameters for Einstein-Hayashi-Shirafuji (EHS) theories of interpolation parameter σ in autoparallel scheme and in extremal scheme. All parameter values are normalized by the physical mass m of the body generating the gravity. The parameter \mathcal{G} and α are related to \mathcal{G}_0 and α_0 in Table III by $\mathcal{G} = \mathcal{G}_0/(1 - \sigma)$ and $\alpha = \alpha_0/(1 - \sigma)$ in autoparallel scheme, $\mathcal{G} = \mathcal{G}_0$ and $\alpha = \alpha_0$ in extremal scheme. The value for \mathcal{G} is set to -2 by the Kerr metric in linear regime $m/r \ll 1$ and $a/r \ll 1$.

	General Relativity	EHS with autoparallels	EHS with extremals
Averaged Geodetic Precession	$(3m/2r_0)\vec{\omega}_O \times \vec{S}_0$	$(1 - 4\tau/3)(3m/2r_0)\vec{\omega}_O \times \vec{S}_0$	$(1 - \sigma - 4\tau/3)(3m/2r_0)\vec{\omega}_O \times \vec{S}_0$
Averaged Frame-dragging	$(I/2r_0^3)\vec{\omega}_E \times \vec{S}_0$	$(-\mathcal{G}/2)(1 - \sigma)(I/2r_0^3)\vec{\omega}_E \times \vec{S}_0$	$(-\mathcal{G}/2)(1 - \sigma)(I/2r_0^3)\vec{\omega}_E \times \vec{S}_0$
Second moment \vec{a}_2	$(3I\omega_E/4r_0^3)\hat{z} \times \vec{S}_0$	$(-3\mathcal{G}I\omega_E/8r_0^3)(1 - \sigma)\hat{z} \times \vec{S}_0$	$(-3\mathcal{G}I\omega_E/8r_0^3)(1 - \sigma)\hat{z} \times \vec{S}_0 - \eta\sigma m\omega_O(S_0^x\hat{z} + S_0^z\hat{x})/4r_0$
Second moment \vec{b}_2	$(3I\omega_E/4r_0^3)\hat{x} \times \vec{S}_0$	$(-3\mathcal{G}I\omega_E/8r_0^3)(1 - \sigma)\hat{x} \times \vec{S}_0$	$(-3\mathcal{G}I\omega_E/8r_0^3)(1 - \sigma)\hat{x} \times \vec{S}_0 - \eta\sigma m\omega_O(S_0^x\hat{x} - S_0^z\hat{z})/4r_0$

TABLE V: Summary of the predicted Fourier moments of the precession rate for General Relativity and the Einstein-Hayashi-Shirafuji (EHS) theories in autoparallel scheme and in extremal scheme. $\eta = +1$ for extremal scheme using $S^{\mu\nu}$, and -1 for extremal scheme using S^μ . Other multiple moments vanish. Here m and $I\omega_E$ are the Earth's mass and rotational angular momentum, respectively.

Effects	Torsion Biases	EHS in autoparallel scheme	EHS in extremal scheme	PPN biases
Shapiro time delay	$\Delta t/\Delta t^{(GR)} = (\mathcal{F} - \mathcal{H})/4$	$1 + \sigma - \tau$	$1 - \tau$	$(1 + \gamma)/2$
Deflection of light	$\delta/\delta^{(GR)} = (\mathcal{F} - \mathcal{H})/4$	$1 + \sigma - \tau$	$1 - \tau$	$(1 + \gamma)/2$
Gravitational redshift	$(\Delta\nu/\nu)/(\Delta\nu/\nu)^{(GR)} = -\mathcal{H}/2$	$1 + \sigma$	1	$1 + \alpha$
Geodetic Precession	$\Omega_G/\Omega_G^{(GR)} = b_t$	$1 - \frac{4}{3}\tau$	$1 - \sigma - \frac{4}{3}\tau$	$(1 + 2\gamma)/3$
Frame-dragging	$\Omega_F/\Omega_F^{(GR)} = b_\mu$	$1 - \sigma$	$1 - \sigma$	$(1 + \gamma + \alpha_1/4)/2$

TABLE VI: Summary of solar system experiments (1): the biases relative to GR predictions for the Einstein-Hayashi-Shirafuji (EHS) theories. Both parameters τ and σ are assumed small. The biases in the PPN formalism are also listed for comparison, taken from [3].

Effects	PPN	EHS in autoparallel scheme	EHS in extremal scheme	Remarks
Shapiro time delay	$\gamma - 1 = (2.1 \pm 2.3) \times 10^{-5}$	$\sigma - \tau = (1.1 \pm 1.2) \times 10^{-5}$	$\tau = (-1.1 \pm 1.2) \times 10^{-5}$	Cassini tracking [122]
Deflection of light	$\gamma - 1 = (-1.7 \pm 4.5) \times 10^{-4}$	$\sigma - \tau = (-0.8 \pm 2.3) \times 10^{-4}$	$\tau = (0.8 \pm 2.3) \times 10^{-4}$	VLBI [123]
Gravitational redshift	$ \alpha < 2 \times 10^{-4}$	$ \sigma < 2 \times 10^{-4}$	no constraints	Vessot-Levine rocket [124]
Geodetic Precession	$ \gamma - 1 < 1.1 \times 10^{-4}$	$ \tau < 5.7 \times 10^{-5}$	$ \sigma + 4\tau/3 < 7.6 \times 10^{-5}$	Gravity Probe B
Frame-dragging	$ \gamma - 1 + \frac{1}{4}\alpha_1 < 0.024$	$ \sigma < 0.012$	$ \sigma < 0.012$	Gravity Probe B

TABLE VII: Summary of solar system experiments (2): constraints on the PPN and EHS parameters. The constraints on PPN parameters are taken from Table 4 and Page 12 of [3]. The full results of Gravity Probe B are yet to be released, so whether the frame dragging will agree with the GR prediction is not currently known. The last two rows show the limits that would correspond to a GPB result consistent with GR, assuming an angle accuracy of 0.5 milli-arcseconds.

There are four parameters c_1 , c_2 , c_3 and σ that define an EHS theory via the action in Eq. (112). We will test EHS theories with GPB and other solar system experiments. For all these weak field experiments, only two EHS parameters — τ (defined in Eq. (113)) and σ , both assumed small — that are functions of the said four are relevant and to be constrained below.

The predicted EHS metric and torsion parameters, studied in Section IX, are listed in Table III. Below, we will test both the autoparallel and extremal calculation schemes. In each scheme, the physical mass m will be determined by the Newtonian limit. All metric and torsion parameters are converted in accordance with m and listed in Table IV. Then the parameter space (τ, σ) will be constrained by solar system experiments.

A. Autoparallel scheme

Hayashi-Shirafuji maximal torsion theory is inconsistent with the autoparallel scheme, since $t_1 - \mathcal{H}/2 = 0$ (see t_1 and \mathcal{H} in Table III). By Eq. (37), this means that $d\vec{v}/dt = 0 + \mathcal{O}(m/r)^2$. The violation of Newton's law rules out the application of the autoparallel scheme to the Hayashi-Shirafuji theory.

However, the Einstein-Hayashi-Shirafuji theories can be consistent with this scheme. Using Table III, the Newtonian limit can be written as

$$\frac{d\vec{v}}{dt} = -(1 - \sigma)\frac{m_0}{r^2}\hat{e}_r, \quad (116)$$

so the physical mass of the central gravitating body is

$$m = (1 - \sigma)m_0. \quad (117)$$

Table IV lists values of metric and torsion parameters in accordance with the physical mass m . Using these parameters, the precession rates of gyroscopes in GPB orbit can be calculated via equations (68),(69),(70) and (73). The results are listed in Table V. For GPB, the average precession rates are the only experimentally accessible observables in practice. GPB will measure the precession of gyroscopes with respect to two different axes: the orbital angular velocity $\vec{\omega}_O$ (geodetic precession) and the Earth's rotational angular velocity $\vec{\omega}_E$ (frame-dragging). As indicated in Table V, the geodetic precession and frame-dragging rates are

$$\Omega_G = (1 - \frac{4}{3}\tau)\Omega_G^{(GR)}, \quad (118)$$

$$\Omega_F = \left(-\frac{\mathcal{G}}{2}\right)(1 - \sigma)\Omega_F^{(GR)}, \quad (119)$$

where $\Omega_G^{(GR)}$ and $\Omega_F^{(GR)}$ are the geodetic precession and frame-dragging rate predicted by General Relativity, respectively.

The existing solar system experiments, including Shapiro time delay, deflection of light, gravitational redshift, advance of Mercury's perihelion, can put constraints on the parameters τ and σ . The derivation of these constraints essentially follow any standard textbook of General Relativity [83] except for more general allowance of parameter values, so we leave the techni-

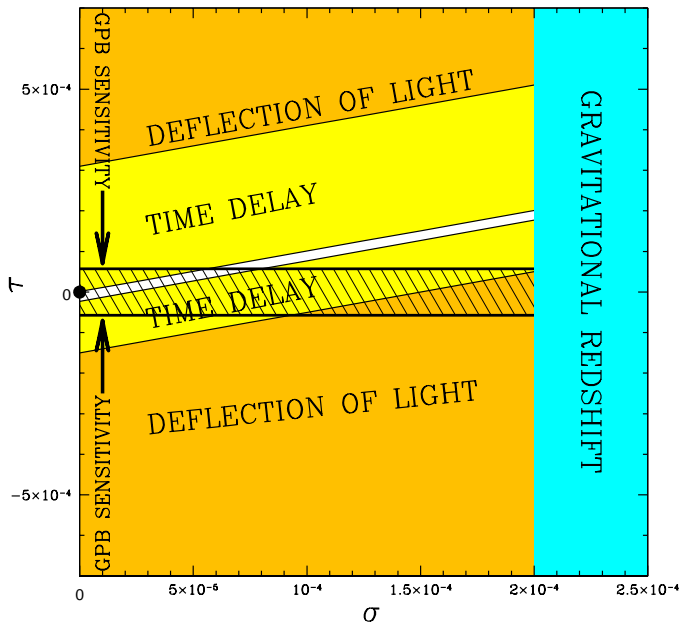


FIG. 4: Constraints on the EHS parameters (σ, τ) from solar system tests in the autoparallel scheme. General Relativity corresponds to the black dot ($\sigma = \tau = 0$). The shaded regions in the parameter space have already been ruled out by Mercury's perihelion shift (red/dark grey), the deflection of light (orange/grey), Shapiro time delay (yellow/light grey) and gravitational redshift (cyan/light grey). If the geodetic precession and frame-dragging measured by Gravity Probe B are consistent with GR to the target accuracy of 0.5 milli-arcseconds, this will rule out everything outside the hatched region, implying that $0 \leq \sigma < 8.0 \times 10^{-5}$ and $-2.3 \times 10^{-5} < \tau < 5.7 \times 10^{-5}$. Preliminary result of Gravity Probe B have only confirmed the geodetic precession to about 1%, thus bringing no further constraints beyond those from gravitational redshift.

cal detail in Appendix C with the results summarized in Table VI.

It is customary that biases of GR predictions are expressed in terms of PPN parameters on which observational constraints can be placed with solar system experiments. In EHS theories, these biases are expressed in terms of the parameters τ and σ . Thus we can place constraints on the EHS parameters τ and σ by setting up the correspondence between PPN and EHS parameters via the bias expression. Table VI lists the biases in the PPN formalism for this purpose, and Table VII lists the observational constraints on the EHS parameters τ and σ with the existing solar system tests.

If GPB would see no evidence of the torsion induced precession effects, the (τ, σ) parameter space can be further constrained. Together with other solar system experiments, the observational constraints are listed in Table VII and shown in Figure 4.

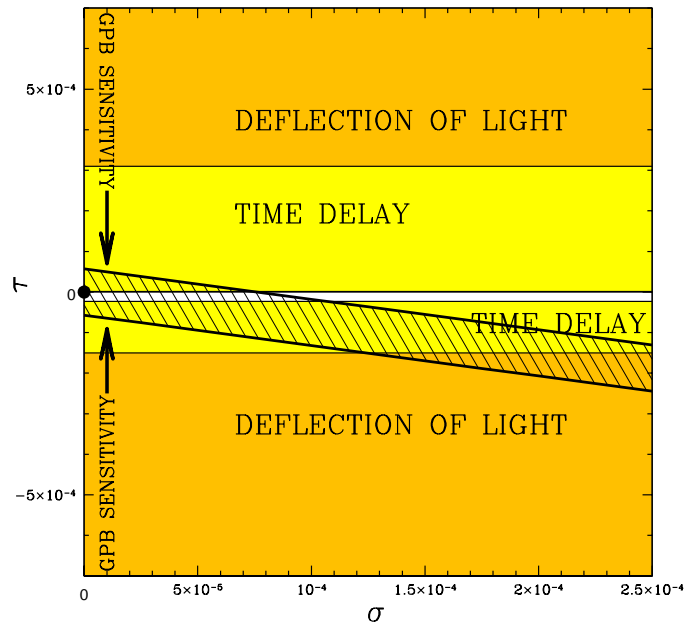


FIG. 5: Constraints on EHS parameters (σ, τ) from solar system tests in the extremal scheme. General Relativity corresponds to the black dot ($\sigma = \tau = 0$). The shaded regions have already been ruled out by Mercury's perihelion shift (red/dark grey), the deflection of light (orange/grey) and Shapiro time delay (yellow/light grey). If the geodetic precession and frame-dragging measured by Gravity Probe B are consistent with GR to the target accuracy of 0.5 milli-arcseconds, this will rule out everything outside the hatched region, implying that $0 \leq \sigma < 1.1 \times 10^{-4}$ and $-2.3 \times 10^{-5} < \tau < 0.1 \times 10^{-5}$. The preliminary result of Gravity Probe B have confirmed the geodetic precession only to about 1%, implying that $\sigma < 0.01$.

B. Extremal scheme

Einstein-Hayashi-Shirafuji theories predict $\mathcal{H} = -2$ regardless of τ and σ . By the Newtonian limit, therefore, the physical mass of the central gravitating body is just the mass parameter m_0 , i.e. $m = m_0$. So the parameter values do not need rescaling and are re-listed in Table IV. By these parameters the precession rates can be calculated and listed in Table V. As indicated in Table V, the geodetic precession and frame-dragging rates are

$$\Omega_G = (1 - \sigma - \frac{4}{3}\tau)\Omega_G^{(GR)}, \quad (120)$$

$$\Omega_F = \left(-\frac{G}{2}\right)(1 - \sigma)\Omega_F^{(GR)}. \quad (121)$$

It is worth noting again that the extremal scheme is not a fully consistent framework from the theoretical point of view. However, it serves perfectly to show the role of EHS theories as the bridge between no-torsion GR and Hayashi-Shirafuji maximal torsion theory. Figure 6 illustrates this connectivity in terms of the predictions of GR, Hayashi-Shirafuji theory and the intermediate $0 < \sigma < 1$

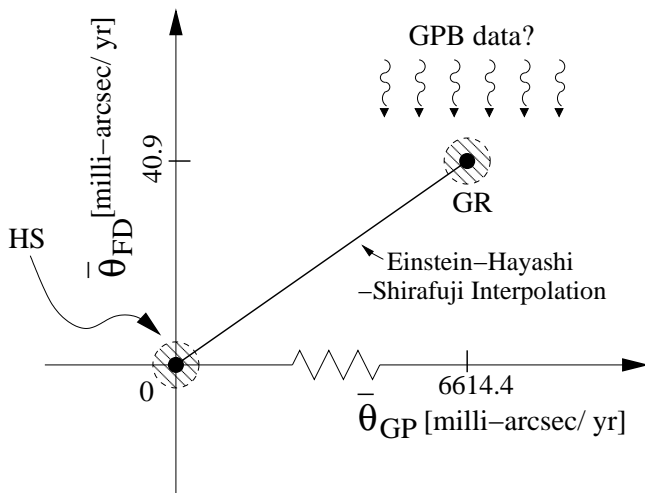


FIG. 6: Predictions for the *average* precession rate by General Relativity, Hayashi-Shirafuji (HS) gravity and Einstein-Hayashi-Shirafuji theories (for the case of $\tau = 0$ and the Kerr solution $\mathcal{G} = -2$) that interpolate between these two extremes, in the extremal scheme. $\bar{\theta}_{GP}$ is the geodetic precession rate around the orbital angular velocity vector $\vec{\omega}_O$ and $\bar{\theta}_{FD}$ is the angular frame-dragging rate around Earth’s rotation axis $\vec{\omega}_E$. The shaded areas of about 0.5 milli-arcseconds per year in radius are the approximate forecast GPB measurement uncertainties. The two calculation schemes using S^μ and $S^{\mu\nu}$ with extremals for the Hayashi-Shirafuji Lagrangian (labeled “HS” in the figure) agree on the predicted average rates. The unpublished preliminary results of Gravity Probe B have confirmed the geodetic precession to better than 1%, so this already rules out the Hayashi-Shirafuji Lagrangian and most EHS theories in the extremal scheme in the sense that $\sigma < 0.01$.

EHS theories, taking $\tau = 0$ and Kerr solution $\mathcal{G} = -2$, on the *average* precession rate (the \bar{a}_0 in Table V). The EHS theories are seen to connect the extreme GR and HS cases with a straight line. If the data released by GPB ends up falling within the shaded area corresponding to the GR prediction, the Hayashi-Shirafuji Lagrangian will thus have been ruled out with very high significance, and the GPB torsion constraints can be quantified as sharp upper limits on the σ -parameter.

More generally, Gravity Probe B will improve the constraints on the (τ, σ) parameter space by its precise measurements of precession rates, in addition to the constraints put by existing solar system experiments. These constraints are listed in Table VII and shown in Figure 5. As before, the technical details are given in Appendix C.

C. Preliminary constraints from GPB’s unpublished results

In April 2007, Gravity Probe B team announced that, while they continued mining the data for the ultimately optimal accuracy, the geodetic precession was found to agree with GR at the 1% level. The frame-dragging yet awaits to be confirmed. Albeit preliminary, these unpublished results, together with solar system tests, already

place the first constraint on some torsion parameters to the 1% level. More quantitatively, $|t_2 + \frac{17}{2}t_1| \lesssim 0.01$ in the model-independent framework, while $w_1 + w_2 - w_3 - 2w_4 + w_5$ is not constrained. In the context of EHS theories, the constraint is scheme dependent. In the autoparallel scheme, GPB’s preliminary results place no better constraints than those from gravitational redshift ($\sim 10^{-4}$). In the extremal scheme, however, the preliminary results give the constraint $\sigma < 0.01$. The bottom line is that GPB has constrained torsion parameters to the 1% level now and will probably reach the 10^{-4} level in the future.

XI. CONCLUSIONS AND OUTLOOK

The PPN formalism has demonstrated that a great way to test GR is to embed it in a broader parametrized class of theories, and to constrain the corresponding parameters observationally. In this spirit, we have explored observational constraints on generalizations of GR including torsion.

Using symmetry arguments, we showed that to lowest order, the torsion field around a uniformly rotating spherical mass such as Earth is determined by merely seven dimensionless parameters. We worked out the predictions for these seven torsion parameters for a two-parameter Einstein-Hayashi-Shirafuji generalization of GR which includes as special cases both standard no-torsion GR ($\sigma = 0$) and the no-curvature, all torsion ($\sigma = 1$) Weitzenböck spacetime. We showed that classical solar system tests rule out a large class of these models, and that Gravity Probe B (GPB) can further improve the constraints. GPB is useful here because this class of theories suggested that, depending on the Lagrangian, rotating objects can generate torsion observable with gyroscopes. In other words, despite some claims in the literature to the contrary, the question of whether there is observable torsion in the solar system is one which ultimately can and should be tested experimentally.

Our results motivate further theoretical and experimental work. On the theoretical side, it would be interesting to address in more detail the question of which Lagrangians make torsion couple to rotating objects. A well-defined path forward would be to generalize the matched asymptotic expansion method of [111, 112] to match two generalized EHS Kerr-like Solutions in the weak-field limit to obtain the laws of motion for two well-separated rotating objects, and determine which of the three non-equivalent prescriptions above, if any, is correct. It would also be interesting to look for generalizations of the EHS Lagrangian that populate a large fraction of the seven torsion degrees of freedom that symmetry allows. Finally, additional observational constraints can be investigated involving, *e.g.*, binary pulsars, gravitational waves and cosmology.

On the experimental side, Gravity Probe B has now successfully completed its data taking phase. We have

shown that the GPB data constitute a potential gold mine of information about torsion, but that its utility for constraining torsion theories will depend crucially on how the data are analyzed and released. At a minimum, the average geodetic and frame dragging precessions can be compared with the predictions shown in Figure 6. However, if it is technically feasible for the GPB team to extract and publish also different linear combinations of the instantaneous precessions corresponding to the second moments of these precessions, this would enable looking for further novel effects that GR predicts should be absent. In summary, although the nominal goal of GPB is to look for an effect that virtually everybody expects will be present (frame dragging), it also has the potential to either discover torsion or to build further confidence in GR by placing stringent limits on torsion theories.

The authors wish to thank Francis Everitt, Thomas Faulkner, Friedrich Hehl, Scott Hughes, Erotokritos Katsavounidis, Barry Muhlfelder, Tom Murphy, Robyn Sanderson, Alexander Silbergleit, Molly Swanson, Takamitsu Tanaka and Martin White for helpful discussions and comments. This work is supported by the U.S. Department of Energy (D.O.E.) under cooperative research agreement DE-FC02-94ER40818, NASA grants NAG5-11099 and NNG06GC55G, NSF grants AST-0134999 and 0607597, and fellowships from the David and Lucile Packard Foundation and the Research Corporation.

APPENDIX A: PARAMETRIZATION OF TORSION IN THE STATIC, SPHERICALLY AND PARITY SYMMETRIC CASE

In this appendix, we derive a parametrization of the most general static, spherically and parity symmetric torsion in isotropic rectangular and spherical coordinates. The symmetry conditions are described in Section III A 1 with the quantity \mathcal{O} now being the torsion tensor $S_{\mu\nu}{}^\rho$. Note that torsion (the antisymmetric part of the connection) is a tensor under general coordinate transformations even though the full connection is not.

First note that time translation invariance is equivalent to the independence of torsion on time. Then consider time reversal, under which a component of torsion flips its sign once for every temporal index. Invariance under time reversal therefore requires that non-zero torsion components have either zero or two temporal indices. Together with the fact that torsion is antisymmetric in its first two indices, this restricts the non-zero components of torsion to be $S_{0i}{}^0$ and $S_{jk}{}^i$ ($i = 1, 2, 3$).

Now consider the symmetry under (proper or improper) rotation (see Eq. (13)). The orthogonality of the matrix \mathbf{R} enables one to write

$$\frac{\partial x^i}{\partial x^j} = R^{ij}, \quad \frac{\partial x^i}{\partial x^j} = R^{ji}, \quad \frac{\partial t'}{\partial t} = \frac{\partial t}{\partial t'} = 1. \quad (\text{A1})$$

Thus formal functional invariance means that

$$\begin{aligned} S'_{0i}{}^0(x') &= R^{ij} S_{0j}{}^0(x) = S_{0i}{}^0(x'), \\ S'_{jk}{}^i(x') &= R^{jm} R^{kn} R^{il} S_{mn}{}^l(x) = S_{jk}{}^i(x'). \end{aligned} \quad (\text{A2})$$

Eq. (A2) requires that the torsion should be built up of x^i and quantities invariant under $O(3)$, such as scalar functions of radius and Kronecker δ -functions, since $\delta'_{i'j'} = R^{i'i} R^{j'j} \delta_{ij} = R^{i'i} R^{j'j} = R^{i'i} (R^{-1})^{j'j} = \delta_{i'j'}$. Note that we are interested in the parity symmetric case, whereas the Levi-Civita symbol ϵ_{ijk} is a three-dimensional *pseudo*-tensor under orthogonal transformations, where “pseudo” means that ϵ_{ijk} is a tensor under $SO(3)$ but not under $O(3)$, since $\epsilon'_{i'j'k'} = R^{i'i} R^{j'j} R^{k'k} \epsilon_{ijk} = \det R \times \epsilon_{i'j'k'}$. Therefore, ϵ_{ijk} is prohibited from entering into the construction of the torsion tensor by Eq. (A2).

Thus using arbitrary combinations of scalar functions of radius, x^i and Kronecker δ -functions, the most general torsion tensor that can be constructed takes the form

$$S_{0i}{}^0 = t_1 \frac{m}{2r^3} x^i, \quad (\text{A3})$$

$$S_{jk}{}^i = t_2 \frac{m}{2r^3} (x^j \delta_{ki} - x^k \delta_{ji}), \quad (\text{A4})$$

where the combinations $t_1 m$ and $t_2 m$ are arbitrary functions of radius. Note that in Eq. (A4), terms proportional to $x^i x^j x^k$ or $x^i \delta_{jk}$ are forbidden by the antisymmetry of the torsion. We will simply treat the functions $t_1(r)$ and $t_2(r)$ as constants, since GPB orbits at a fixed radius.

Transforming this result to spherical coordinates, we obtain

$$\begin{aligned} S_{tr}{}^t &= S_{ti}{}^t \frac{\partial x^i}{\partial r} = t_1 \frac{m}{2r^2}, \\ S_{r\theta}{}^\theta &= S_{jk}{}^i \frac{\partial x^j}{\partial r} \frac{\partial x^k}{\partial \theta} \frac{\partial \theta}{\partial x^i} = t_2 \frac{m}{2r^2}, \\ S_{r\phi}{}^\phi &= S_{jk}{}^i \frac{\partial x^j}{\partial r} \frac{\partial x^k}{\partial \phi} \frac{\partial \phi}{\partial x^i} = t_2 \frac{m}{2r^2}. \end{aligned}$$

All other components not related by the antisymmetry vanish. In the above equations, the second equalities follow from the chain rule and the facts that $\partial x^i / \partial r = \hat{x}^i = \hat{e}_r^i$, $\partial x^i / \partial \theta = r \hat{e}_\theta^i$, and $\partial x^i / \partial \phi = r \sin \theta \hat{e}_\phi^i$, where \hat{e}_r^i , \hat{e}_θ^i and \hat{e}_ϕ^i are the i th-components of the unit vectors in spherical coordinates. To first order in the mass m of the central object, we need not distinguish between isotropic and standard spherical coordinates.

APPENDIX B: PARAMETRIZATION IN STATIONARY AND SPHERICALLY AXISYMMETRIC CASE

Above we considered the 0 th order contribution to the metric and torsion corresponding to the static, spherically and parity symmetric case of a non-rotating spherical source. In this appendix, we derive a parametrization

of the most general 1st order correction (denoted by a superscript (1)) to this metric and torsion that could be caused by rotation of the source, i.e. corresponding to the stationary and spherically axisymmetric case. The symmetry conditions are described in Section III B 1, with the quantity \mathcal{O} replaced by the metric $g_{\mu\nu}^{(1)}$ for Appendix B 1 and by the torsion $S_{\mu\nu}^{(1)\rho}$ for Appendix B 2.

1. The Metric

The invariance under time translation makes the metric time independent. Under time reversal $\mathbf{J} \rightarrow -\mathbf{J}$, and a component of the metric flips its sign once for every temporal index. Thus, the formal functional invariance equation for time reversal reads

$$\pm g_{\mu\nu}^{(1)}(x|\mathbf{J}) = g_{\mu\nu}^{(1)}(x|-\mathbf{J}). \quad (\text{B1})$$

The plus sign in Eq. (B1) is for components with even numbers of temporal indices, and minus sign for those with odd numbers. Since only terms linear in $J/r^2 = \varepsilon_m \varepsilon_a$ are concerned, the minus sign in the argument $-\mathbf{J}$ can be taken out as an overall factor, implying that the non-vanishing components of metric can have only one temporal index. Thus the only nonzero first-order correction to $g_{\mu\nu}$ in rectangular coordinates is $g_{ti}^{(1)}$ ($i=1,2,3$).

Now consider the transformation property under (proper or improper) rotation. By the orthogonality of the matrix \mathbf{R} , the vector \mathbf{x} transforms as $\mathbf{x} \rightarrow \mathbf{x}' \equiv \mathbf{R}\mathbf{x}$ (Eq. (A1)). Since \mathbf{J} is invariant under parity, formally the transformation of \mathbf{J} writes as

$$\mathbf{J} \rightarrow \mathbf{J}' = (\det \mathbf{R}) \times \mathbf{R}\mathbf{J}. \quad (\text{B2})$$

The formal functional invariance for rotation reads

$$g_{ti}^{(1)'}(x'|\mathbf{J}') = R^{ij} g_{tj}^{(1)}(x|\mathbf{J}) = g_{ti}^{(1)}(x'|\mathbf{J}'). \quad (\text{B3})$$

That \mathbf{J} is a pseudo-vector under improper rotation requires that the Levi-Civita symbol ϵ_{ijk} , also a pseudo-tensor, appear once and only once (because \mathbf{J} appears only once) in the metric so as to compensate the $\det \mathbf{R}$ factor incurred by transformation of \mathbf{J} . Other possible elements for construction of the metric include scalar functions of radius, x^i , J^i , δ_{ij} . Having known the elements, the only possible construction is therefore

$$g_{ti}^{(1)} = \frac{\mathcal{G}}{r^2} \epsilon_{ijk} J^j \hat{x}^k, \quad (\text{B4})$$

where $\hat{x}^i = x^i/r$ is the unit vector of position vector and \mathcal{G} is dimensionless. Assuming that there is no new scale other than the angular momentum \mathbf{J} built into the 1st order of torsion theory, i.e. no new dimensional parameter with units of length, $\mathcal{G}(r)$ must be a constant by dimensional analysis, since the factor J^i has explicitly appeared.

In spherical polar coordinates where the z -axis is parallel to \mathbf{J} , this first-order correction to the metric takes the form

$$g_{t\phi}^{(1)} = \mathcal{G} \frac{ma}{r} \sin^2 \theta, \quad (\text{B5})$$

where $ma = J$ is the magnitude of \mathbf{J} . All other components vanish.

2. The Torsion

We follow the same methodology as for our parametrization of the metric above. Given the time-independence, the property that \mathbf{J} reverses under time-reversal requires that the non-vanishing components of torsion have only one temporal index, so they are $S_{ij}^{(1)t}$, $S_{tij}^{(1)}$ ($i,j=1,2,3$) in rectangular coordinates. (The antisymmetry of torsion over its first two indices excludes the possibility of three temporal indices.) Under (proper or improper) rotation, the formal functional invariance equation reads

$$\begin{aligned} S_{ij}^{(1)'}{}^t(x'|\mathbf{J}') &= R^{ik} R^{jl} S_{kl}^{(1)t}(x|\mathbf{J}) = S_{ij}^{(1)'}{}^t(x'|\mathbf{J}'), \\ S_{tij}^{(1)'}(x'|\mathbf{J}') &= R^{ik} R^{jl} S_{tkl}^{(1)}(x|\mathbf{J}) = S_{tij}^{(1)'}(x'|\mathbf{J}'). \end{aligned}$$

Again, in building the torsion, one should use the Levi-Civita symbol ϵ_{ijk} once and only once to cancel the $\det \mathbf{R}$ factor from the transformation of \mathbf{J} . The most general construction using scalar function of radius, x^i , δ_{ij} , J^i (also appearing once and only once) and ϵ_{ijk} is

$$\begin{aligned} S_{ij}^{(1)'}{}^t &= \frac{f_1}{2r^3} \epsilon_{ijk} J^k + \frac{f_2}{2r^3} J^k \hat{x}^l (\epsilon_{ikl} \hat{x}^j - \epsilon_{jkl} \hat{x}^i), \\ S_{tij}^{(1)'} &= \frac{f_3}{2r^3} \epsilon_{ijk} J^k + \frac{f_4}{2r^3} J^k \hat{x}^l \epsilon_{ikl} \hat{x}^j + \frac{f_5}{2r^3} J^k \hat{x}^l \epsilon_{jkl} \hat{x}^i. \end{aligned}$$

By the same dimensional argument as in Appendix (B 1), f_1, \dots, f_5 must be dimensionless constants.

Transforming the above equations to spherical coordinates where the z -axis is parallel to \mathbf{J} , we obtain to first order

$$\begin{aligned} S_{r\phi}^{(1)'}{}^t &= S_{ij}{}^t \frac{\partial x^i}{\partial r} \frac{\partial x^j}{\partial \phi} = w_1 \frac{ma}{2r^2} \sin^2 \theta, \\ S_{\theta\phi}^{(1)'}{}^t &= S_{ij}{}^t \frac{\partial x^i}{\partial \theta} \frac{\partial x^j}{\partial \phi} = w_2 \frac{ma}{2r} \sin \theta \cos \theta, \\ S_{t\phi}^{(1)'}{}^r &= g^{rr} S_{tij} \frac{\partial x^i}{\partial \phi} \frac{\partial x^j}{\partial r} = w_3 \frac{ma}{2r^2} \sin^2 \theta, \\ S_{t\phi}^{(1)'}{}^\theta &= g^{\theta\theta} S_{tij} \frac{\partial x^i}{\partial \phi} \frac{\partial x^j}{\partial \theta} = w_4 \frac{ma}{2r^3} \sin \theta \cos \theta, \\ S_{tr}^{(1)'}{}^\phi &= g^{\phi\phi} S_{tij} \frac{\partial x^i}{\partial r} \frac{\partial x^j}{\partial \phi} = w_5 \frac{ma}{2r^4}, \\ S_{t\theta}^{(1)'}{}^\phi &= g^{\phi\phi} S_{tij} \frac{\partial x^i}{\partial \theta} \frac{\partial x^j}{\partial \phi} = -w_4 \frac{ma}{2r^3} \cot \theta. \end{aligned}$$

All other components vanish. The constants are related by $w_1 = f_1 - f_2$, $w_2 = f_1$, $w_3 = f_4 - f_3$, $w_4 = -f_3$, $w_5 = f_5 + f_3$.

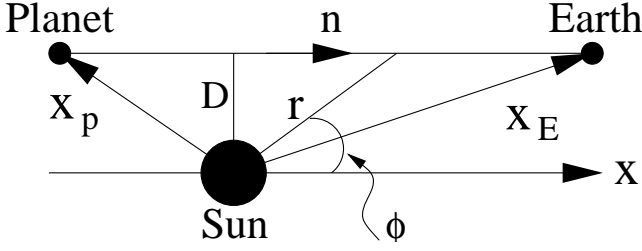


FIG. 7: Geometry of the Shapiro time delay measurement.

APPENDIX C: CONSTRAINING TORSION WITH SOLAR SYSTEM EXPERIMENTS

1. Shapiro time delay

For the electromagnetic field, if torsion is coupled to the vector potential A_μ by the “natural” extension, i.e. $\partial_\mu A_\nu \rightarrow \nabla_\mu A_\nu$ using the full connection, the Maxwell Lagrangian $-\frac{1}{4}F_{\mu\nu}F^{\mu\nu}$ will contain a quadratic term in A_μ that makes the photon massive and breaks gauge invariance in the conventional form. Since the photon mass has been experimentally constrained to be $\lesssim 10^{-17}$ eV, we assume that A_μ does not couple to torsion. Instead, we assume that the Maxwell field Lagrangian in the curved spacetime with torsion follows the extension $\partial_\mu A_\nu \rightarrow \nabla_\mu^{\{\}} A_\nu$ using the Levi-Civita connection. Since the Levi-Civita connection depends on the metric and its derivatives only, light rays follow extremal curves (metric geodesics).

In general, assume the line element in the field around a (physical) mass m is

$$ds^2 = - \left[1 + \mathcal{H} \frac{m}{r} \right] dt^2 + \left[1 + \mathcal{F} \frac{m}{r} \right] dr^2 + r^2 d\Omega^2. \quad (\text{C1})$$

The effect of the rotation of the mass can be ignored when the rotation is slow.

Light deflection angle is tiny for the solar system tests we consider, so a ray can be well approximated by a straight line. Let us use coordinates where the Sun (of mass m), the Earth and a planet reflecting the light ray are all in the x - y plane ($\theta = \pi/2$) and the x -axis points along the ray from the planet to Earth (see Figure 7). Let D be the minimal distance of the ray from the Sun. Then $r \sin \phi = D$, or $rd\phi = -\tan \phi dr$. Since $ds^2 = 0$ for a light ray,

$$\begin{aligned} dt^2 &= (1 + \mathcal{H} \frac{m}{r})^{-1} (1 + \mathcal{F} \frac{m}{r} + \tan^2 \phi) dr^2 \\ &\approx \frac{r^2 dr^2}{r^2 - D^2} \left[1 + (\mathcal{F} - \mathcal{H}) \frac{m}{r} - \mathcal{F} \frac{m D^2}{r^3} \right], \\ dt &\approx \frac{r |dr|}{\sqrt{r^2 - D^2}} \left[1 + (\mathcal{F} - \mathcal{H}) \frac{m}{2r} - \mathcal{F} \frac{m D^2}{2r^3} \right]. \quad (\text{C2}) \end{aligned}$$

The round-trip travel time for an electromagnetic signal bouncing between Earth and the Planet in the gravita-

tional field of the Sun is

$$\begin{aligned} T &= 2 \left[\int_{r=D_p}^{r=D} dt + \int_{r=D}^{r=D_E} dt \right], \\ &\approx 2 \left[\sqrt{D_p^2 - D^2} + \sqrt{D_E^2 - D^2} \right] + (\mathcal{F} - \mathcal{H})m \\ &\quad \times \ln \left[\frac{(\sqrt{D_p^2 - D^2} + D_p)(\sqrt{D_E^2 - D^2} + D_E)}{D^2} \right] \\ &\quad - \mathcal{F}m \left(\frac{\sqrt{D_p^2 - D^2}}{D_p} + \frac{\sqrt{D_E^2 - D^2}}{D_E} \right). \quad (\text{C3}) \end{aligned}$$

If $D \ll D_E$ and $D \ll D_p$, the third term in Eq. (C3) is negligible compared to the second one. The excess travel time Δt of a round-trip light ray is

$$\begin{aligned} \Delta t &\equiv T - 2 \left[\sqrt{D_p^2 - D^2} + \sqrt{D_E^2 - D^2} \right], \\ &\approx \left(\frac{\mathcal{F} - \mathcal{H}}{4} \right) \Delta t^{(GR)}, \quad (\text{C4}) \end{aligned}$$

where $\Delta t^{(GR)}$ is the excess time predicted by GR

$$\Delta t^{(GR)} = 4m \ln \left[\frac{(D_E + \vec{x}_E \cdot \hat{n})(D_p - \vec{x}_p \cdot \hat{n})}{D^2} \right]. \quad (\text{C5})$$

Here \vec{x}_E (\vec{x}_p) is the vector from the Sun to the Earth (the planet), and \hat{n} is the unit vector from the planet to Earth (see Figure 7).

For EHS theories in the autoparallel scheme, $(\mathcal{F} - \mathcal{H})/4 = (1 - \epsilon)/(1 - \sigma) \approx 1 + \sigma - \epsilon$, if $\sigma \ll 1$. For EHS theories in the extremal scheme, $(\mathcal{F} - \mathcal{H})/4 = 1 - \epsilon$.

2. Deflection of light

As discussed in Appendix C1, we assume that a light ray follows an extremal curve (metric geodesic), taking the form

$$\frac{D^{\{\}} u^\mu}{D\tau} = \frac{d^2 x^\mu}{d\tau^2} + \left\{ \begin{array}{c} \mu \\ \nu\rho \end{array} \right\} \frac{dx^\nu}{d\tau} \frac{dx^\rho}{d\tau} = 0. \quad (\text{C6})$$

Here $D^{\{\}}/D\tau$ denotes the covariant differentiation using the Levi-Civita connection.

The $\mu = t$ component of the metric geodesic is

$$\frac{d^2 t}{d\tau^2} - \mathcal{H} \frac{m}{r^2} \frac{dt}{d\tau} \frac{dr}{d\tau} = 0,$$

or, to order $\mathcal{O}(m/r)$, where m is the mass of the Sun deflecting the light,

$$\frac{d}{d\tau} \left[\left(1 + \mathcal{H} \frac{m}{r} \right) \frac{dt}{d\tau} \right] = 0.$$

Integrating this gives a conserved quantity,

$$k \equiv \left(1 + \mathcal{H} \frac{m}{r} \right) \frac{dt}{d\tau} = \text{const}. \quad (\text{C7})$$

The $\mu = \theta$ component of the metric geodesic admits the planar solution $\theta = \pi/2$. The $\mu = \phi$ component of the metric geodesic, when $\theta = \pi/2$, is

$$\frac{d^2\phi}{d\tau^2} + \frac{2}{r} \frac{dr}{d\tau} \frac{d\phi}{d\tau} = 0,$$

whose first integral gives another conserved quantity,

$$h \equiv r^2 \frac{d\phi}{d\tau} = \text{const}. \quad (\text{C8})$$

For light rays in the equatorial plane $\theta = \pi/2$,

$$\frac{ds^2}{d\tau^2} = - \left[1 + \mathcal{H} \frac{m}{r} \right] \left(\frac{dt}{d\tau} \right)^2 + \left[1 + \mathcal{F} \frac{m}{r} \right] \left(\frac{dr}{d\tau} \right)^2 + r^2 \left(\frac{d\phi}{d\tau} \right)^2 = 0. \quad (\text{C9})$$

Note that the $\mu = r$ component of the metric geodesic is not independent of Eq. (C9). Rewriting $dt/d\tau$ and $d\phi/d\tau$ in terms of k and h via Eq. (C20) and Eq. (C21), respectively, and using the fact that $dr/d\tau = (dr/d\phi)(d\phi/d\tau)$, one finds

$$\frac{d^2u}{d\phi^2} + u = \frac{3}{2} \mathcal{F} m u^2 - \frac{k^2}{h^2} \frac{\mathcal{F} + \mathcal{H}}{2} m, \quad (\text{C10})$$

where $u \equiv 1/r$. The solution to order $\mathcal{O}(m)$ is

$$u = \frac{\sin\phi}{D} + \frac{\mathcal{F}m}{2D^2} (1 + C \cos\phi + \cos^2\phi) - \frac{k^2}{h^2} \frac{\mathcal{F} + \mathcal{H}}{2} m, \quad (\text{C11})$$

where D is the minimal distance of the ray to the Sun. The x -axis is set up to be along the incoming direction of the ray. C is an arbitrary constant that can be determined at $\phi = \pi$ (incoming infinity). As long as deflection angle $\delta \ll 1$,

$$\delta \simeq \frac{2\mathcal{F}m}{D} - \frac{k^2}{h^2} m (\mathcal{F} + \mathcal{H}) D. \quad (\text{C12})$$

Using

$$\frac{h}{k} = r^2 \frac{d\phi}{dt} \left(1 - \mathcal{H} \frac{m}{r} \right) \approx r^2 \frac{d\phi}{dt} = D \quad (\text{C13})$$

is the angular momentum of the light ray relative to the Sun, we finally obtain

$$\delta \simeq \frac{\mathcal{F} - \mathcal{H}}{4} \delta^{(GR)}, \quad (\text{C14})$$

where $\delta^{(GR)} = 4m/D$ is the deflection angle predicted by GR to lowest order.

3. Gravitational Redshift

As discussed above, we assume that the orbits of light rays are metric geodesics even when there is non-zero torsion. Non-relativistically, the metric geodesic equation for a test particle is

$$\frac{d\vec{v}}{dt} = - \frac{(-\mathcal{H})}{2} \frac{m}{r^2} \hat{e}_r. \quad (\text{C15})$$

Effectively this introduces the gravitational potential U , defined by $d\vec{v}/dt = \vec{F} \equiv -\nabla U$,

$$U = - \frac{(-\mathcal{H})}{2} \frac{m}{r}. \quad (\text{C16})$$

Thus the gravitational redshift of photons is

$$\frac{\Delta\nu}{\nu} = \frac{(-\mathcal{H})}{2} \left(\frac{\Delta\nu}{\nu} \right)^{(GR)}, \quad (\text{C17})$$

where $(\Delta\nu/\nu)^{(GR)}$ is the redshift predicted by GR

$$\left(\frac{\Delta\nu}{\nu} \right)^{(GR)} = - \frac{m}{c^2} \left(\frac{1}{r_1} - \frac{1}{r_2} \right). \quad (\text{C18})$$

For EHS theories in the autoparallel scheme, $-\mathcal{H}/2 = 1/(1-\sigma) \approx 1+\sigma$ for $\sigma \ll 1$. For EHS theories in extremal scheme, $-\mathcal{H}/2 = 1$ exactly.

4. Advance of Mercury's Perihelion in autoparallel scheme

In the autoparallel scheme, a massive test particle (*e.g.* a planet in the field of the Sun) follows an autoparallel curve (*i.e.* an affine geodesic). We now derive the advance of the perihelion when torsion is present. The autoparallel equation reads

$$\frac{Du^\mu}{D\tau} = \frac{d^2x^\mu}{d\tau^2} + \Gamma^\mu_{\nu\rho} \frac{dx^\nu}{d\tau} \frac{dx^\rho}{d\tau} = 0, \quad (\text{C19})$$

where $D/D\tau$ is the covariant differentiation by the full connection.

The $\mu = t$ component of Eq. (C19) reads

$$\frac{d^2t}{d\tau^2} + (t_1 - \mathcal{H}) \frac{m}{r^2} \frac{dt}{d\tau} \frac{dr}{d\tau} = 0,$$

or, to order $\mathcal{O}(m/r)$, where m is the mass of the central gravitating body (*e.g.* the Sun),

$$\frac{d}{d\tau} \left[\left(1 + (\mathcal{H} - t_1) \frac{m}{r} \right) \frac{dt}{d\tau} \right] = 0.$$

The integral gives a conserved quantity k ,

$$k \equiv \left(1 + (\mathcal{H} - t_1) \frac{m}{r} \right) \frac{dt}{d\tau} = \text{const}. \quad (\text{C20})$$

The $\mu = \theta$ component of Eq. (C19) admits the planar solution $\theta = \pi/2$. The $\mu = \phi$ component of Eq. (C19), when $\theta = \pi/2$, is

$$\frac{d^2\phi}{d\tau^2} + \left(\frac{2}{r} - t_2 \frac{m}{r^2} \right) \frac{dr}{d\tau} \frac{d\phi}{d\tau} = 0,$$

whose first integral gives another conserved quantity h ,

$$h \equiv r^2 \frac{d\phi}{d\tau} \left(1 + t_2 \frac{m}{r} \right) = \text{const}. \quad (\text{C21})$$

The path parameter τ can be chosen so that

$$ds^2/d\tau^2 = g_{\mu\nu} \frac{dx^\mu}{d\tau} \frac{dx^\nu}{d\tau} = -1. \quad (\text{C22})$$

Eq. (C22) is consistent with the autoparallel scheme since $\nabla_\rho g_{\mu\nu} = 0$ and $Du^\mu/D\tau = 0$. Note that the $\mu = r$ component of Eq. (C19) is not independent of Eq. (C22). For a test particle in the equatorial plane $\theta = \pi/2$, Eq. (C22) reads

$$-\left[1 + \mathcal{H} \frac{m}{r}\right] \left(\frac{dt}{d\tau}\right)^2 + \left[1 + \mathcal{F} \frac{m}{r}\right] \left(\frac{dr}{d\tau}\right)^2 + r^2 \left(\frac{d\phi}{d\tau}\right)^2 = -1. \quad (\text{C23})$$

Reusing the trick employed in Appendix C 2, we find

$$\frac{d^2u}{d\phi^2} + u = \frac{3}{2} \mathcal{F} m u^2 + \frac{m}{2h^2} [k^2(-\mathcal{H} - \mathcal{F} + 2t_1 + 2t_2) + \mathcal{F} - 2t_2], \quad (\text{C24})$$

to order $\mathcal{O}(mu)$, where $u \equiv 1/r$. Note that to lowest order $k \approx 1 + \mathcal{O}(m, (\text{velocity})^2)$, so the second term on the right hand side of Eq. (C24) becomes $(t_1 - \mathcal{H}/2)m/h^2$. Since m is the physical mass of the central gravitating body, the autoparallel scheme requires $t_1 - \mathcal{H}/2 = 1$. Now Eq. (C24) becomes

$$\frac{d^2u}{d\phi^2} + u = \frac{m}{h^2} + \frac{3}{2} \mathcal{F} m u^2. \quad (\text{C25})$$

Solve the equation perturbatively in the order of $\varepsilon \equiv (m/h)^2$, i.e. use the ansatz $u = u_0 + \varepsilon u_1$. One finds

$$u_0 = \frac{m}{h^2} (1 + e \cos \phi) \quad (\text{C26})$$

$$u_1 = \frac{3\mathcal{F}m}{2h^2} \left[1 + e\phi \sin \phi + \frac{e^2}{2} \left(1 - \frac{1}{3} \cos 2\phi \right) \right] \quad (\text{C27})$$

Eq. (C26) gives the classical elliptical orbit with eccentricity e and the semi-latus rectum $p \equiv a(1 - e^2) = h^2/m$. The $\phi \sin \phi$ term in Eq. (C27) contributes to the advance of the perihelion, while the constant and $\cos 2\phi$ terms do not. Therefore

$$u \approx \frac{m}{h^2} \left\{ 1 + e \cos \left[\phi \left(1 - \frac{3\mathcal{F}m^2}{2h^2} \right) \right] \right\}. \quad (\text{C28})$$

In Eq. (C28), we used the fact that the second term inside the cosine is $\ll 1$. The advance of the perihelion is now given by

$$\begin{aligned} \Delta\theta &= \frac{2\pi}{1 - \frac{3\mathcal{F}m^2}{2h^2}} - 2\pi \\ &= \frac{\mathcal{F}}{2} \Delta\theta^{(GR)}, \end{aligned} \quad (\text{C29})$$

where $\Delta\theta^{(GR)} = 6\pi m^2/h^2 = 6\pi m/p$ is the perihelion advance predicted by GR.

5. Advance of Mercury's Perihelion in extremal scheme

The extremal scheme assumes that a test particle (*e.g.*, a planet) follows the metric geodesic even though the torsion is present. Following the same algebra as in Appendix C 4, and noting that $\mathcal{H} = -2$ for the extremal scheme, we find that the advance of the perihelion in the extremal scheme has the same bias factor $\mathcal{F}/2$, i.e., Eq. (C29) holds.

APPENDIX D: CONSTRAINING TORSION PARAMETERS WITH THE UPPER BOUNDS ON THE PHOTON MASS

In this Appendix, we derive the constraints on torsion parameters that result from assuming that the ‘‘natural’’ extension $\partial_\mu \rightarrow \nabla_\mu$ (using the full connection) in the electromagnetic Lagrangian. This breaks gauge invariance, and the photon generically gains a mass via an additional term of the form $-\frac{1}{2}m_\gamma^2 g^{\mu\nu} A_\mu A_\nu$ in the Lagrangian as we will now show. The assumption gives

$$F_{\mu\nu} \equiv \nabla_\mu A_\nu - \nabla_\nu A_\mu = f_{\mu\nu} - 2S_{\mu\nu}{}^\lambda A_\lambda, \quad (\text{D1})$$

where $f_{\mu\nu} \equiv \partial_\mu A_\nu - \partial_\nu A_\mu$. The Maxwell Lagrangian therefore becomes

$$\begin{aligned} \mathcal{L}_{\text{EM}} &= -\frac{1}{4} g^{\mu\alpha} g^{\nu\beta} F_{\mu\nu} F_{\alpha\beta}, \\ &= -\frac{1}{4} g^{\mu\alpha} g^{\nu\beta} f_{\mu\nu} f_{\alpha\beta} - K^{\mu\nu} A_\mu A_\nu + S^{\mu\nu\lambda} A_\lambda f_{\mu\nu}, \end{aligned} \quad (\text{D2})$$

where $K^{\mu\nu} \equiv S_{\alpha\beta}{}^\mu S^{\alpha\beta\nu}$. The Euler-Lagrange equation for the action $S = \int d^4x \sqrt{-g} \mathcal{L}_{\text{EM}}$ yields the following equation of motion for A_μ :

$$\nabla_\mu^\Gamma f^{\mu\nu} = 2S_{\mu\lambda}{}^\mu f^{\lambda\nu} + 2K^{\lambda\nu} A_\lambda + 2\nabla_\mu^{\{\}} (S^{\mu\nu\lambda} A_\lambda). \quad (\text{D3})$$

Here ∇_μ^Γ and $\nabla_\mu^{\{\}}$ are the covariant derivative w.r.t. the full connection and the Levi-Civita connection, respectively. Both the 2nd and 3rd terms on the right hand side of Eq. (D3) contain the coupling to A_μ . To clarify this, Eq. (D3) can be rewritten non-covariantly as

$$\begin{aligned} \nabla_\mu^\Gamma f^{\mu\nu} &= 2S_{\mu\lambda}{}^\mu f^{\lambda\nu} + 2A_\lambda [K^{\lambda\nu} + \partial_\mu S^{\mu\nu\lambda} \\ &\quad + \left\{ \begin{array}{c} \alpha \\ \alpha\mu \end{array} \right\} S^{\mu\nu\lambda}] + 2S^{\mu\nu\lambda} \partial_\mu A_\lambda, \end{aligned} \quad (\text{D4})$$

in which the 2nd term on the right hand side is the direct coupling of A_μ .

The matrix $K^{\mu\nu}$ is symmetric. If it is also positive definitive up to the metric signature $(-+++)$, the first term in the square bracket may be identified as the photon mass term. In the field of a non-rotating mass, using

the parametrization (Eqs. 14 and 15), it can be shown that

$$K^{00} = -\frac{t_1^2 m^2}{2r^4}, \quad (\text{D5})$$

$$K^{0i} = 0, \quad (\text{D6})$$

$$K^{ij} = \frac{t_2^2 m^2}{2r^4} \left(\delta_{ij} - \frac{x^i x^j}{r^2} \right). \quad (\text{D7})$$

The matrix K has the eigenvalues $-\frac{t_1^2 m^2}{2r^4}$, 0 (with eigenvector \hat{r}) and $\frac{t_2^2 m^2}{2r^4}$ (with 2 degenerate eigenvectors). Since the metric signature is $(-+++)$, all photon masses are positive or zero, The nonzero ones are of order

$$m_\gamma \simeq t \frac{m}{r^2}, \quad (\text{D8})$$

or (with units reinserted)

$$m_\gamma c^2 \simeq t \frac{\hbar G m}{c r^2}. \quad (\text{D9})$$

Here $t = \max(|t_1|, |t_2|)$ and r is the distance of the experiment location to the center of the mass m that generates the torsion. For a ground-based experiment here on Earth, this gives

$$t \simeq 4.64 \times 10^{22} m_\gamma c^2 / (1 \text{ eV}). \quad (\text{D10})$$

The upper bound on the photon mass from ground-based experiments is $m_\gamma c^2 < 10^{-17} \text{ eV}$ [125], so the constraint

that this bound places on the dimensionless torsion parameters is quite weak.

Experimentalists can also search for an anomalous electromagnetic force and translate the null results into photon mass bounds. To leading order, the anomalous force is $2\partial_\mu S^{\mu\nu\lambda} A_\lambda$, since the K-term is proportional to S^2 , while the 2nd term in the square bracket of Eq. (D4) is proportional to S . In a field of a non-rotating mass m ,

$$(\partial_\mu S^{\mu\nu\lambda})^{00} = (\partial_\mu S^{\mu\nu\lambda})^{0i} = (\partial_\mu S^{\mu\nu\lambda})^{i0} = 0, \quad (\text{D11})$$

$$(\partial_\mu S^{\mu\nu\lambda})^{ij} = t_2 \frac{m}{2r^3} \left(-\delta_{ij} + 3 \frac{x^i x^j}{r^2} \right), \quad (\text{D12})$$

which has eigenvalues $\frac{t_2 m}{2r^3} \times (0, -1, -1, 2)$. This cannot be identified as a mass term since there must be a negative ‘‘mass squared’’ regardless of the sign of t_2 . However, the anomalous electromagnetic force expressed as a photon mass can be estimated as

$$m_\gamma c^2 \simeq \sqrt{|t_2| \hbar^2 G \frac{m}{r^3}}, \quad (\text{D13})$$

or

$$\sqrt{|t_2|} \simeq 1.23 \times 10^{18} m_\gamma c^2 / \text{eV}. \quad (\text{D14})$$

This implies that current ground-based experimental upper bounds on the photon mass are too weak (giving merely $|t| \lesssim 10^2$, as compared to $|t| = 1$ from Hayashi-Shirafuji gravity) to place constraints on torsion parameters that are competitive with those from GPB.

-
- [1] C. M. Will, *Annalen Phys.* **15**, 19 (2005)
[2] C. M. Will, *Theory and Experiment in Gravitational Physics*, Cambridge University Press (1993).
[3] C. M. Will, gr-qc/0510072.
[4] R. A. Hulse and J. H. Taylor, *Astrophys. J.* **195**, L51 (1975)
[5] J. M. Weisberg and J. H. Taylor, astro-ph/0205280.
[6] J. M. Weisberg and J. H. Taylor, astro-ph/0407149.
[7] D. J. Champion, *et al.*, *Mon. Not. Roy. Astron. Soc.* **350**, L61 (2004)
[8] P. C. Peters and J. Mathews, *Phys. Rev.* **131**, 435 (1963)
[9] I. H. Stairs *et al.*, astro-ph/9712296.
[10] I. H. Stairs, S. E. Thorsett, J. H. Taylor and Z. Arzoumanian, astro-ph/9911198.
[11] A. W. Hotan, M. Bailes and S. M. Ord, *Mon. Not. Roy. Astron. Soc.* **355**, 941 (2004)
[12] A. W. Hotan, M. Bailes and S. M. Ord, *Astrophys. J.* **624**, 906 (2005)
[13] W. van Straten, *et al.*, *Nature* **412**, 158 (2001)
[14] P. J. Armitage, *Astrophys. Space Sci.* **308**, 89 (2004)
[15] S. K. Chakrabarti, astro-ph/0402562.
[16] A. Merloni, astro-ph/0210251.
[17] K. Menou, astro-ph/0111469.
[18] P. Peldan, *Class. Quant. Grav.* **11**, 1087 (1994)
[19] T. P. Sotiriou, gr-qc/0604028.
[20] T. P. Sotiriou and S. Liberati, gr-qc/0604006.
[21] T. P. Sotiriou, *Class. Quant. Grav.* **23**, 1253 (2006)
[22] M. Akbar and R. G. Cai, *Phys. Lett. B* **635**, 7 (2006)
[23] T. Koivisto, *Phys. Rev. D* **73**, 083517 (2006)
[24] M. Amarzguioui, O. Elgaroy, D. F. Mota and T. Multamaki, astro-ph/0510519.
[25] J. c. Hwang and H. Noh, *Phys. Lett. B* **506**, 13 (2001)
[26] X. H. Meng and P. Wang, *Phys. Lett. B* **584**, 1 (2004)
[27] G. Esposito-Farese, gr-qc/9903058.
[28] G. Esposito-Farese, *AIP Conf. Proc.* **736**, 35 (2004)
[29] T. Damour, gr-qc/9606079.
[30] D. Puetzfeld, *New Astron. Rev.* **49**, 59 (2005)
[31] U. Kasper, S. Kluske, M. Rainer, S. Reuter and H. J. Schmidt, gr-qc/9410030.
[32] S. Biswas, A. Shaw and D. Biswas, gr-qc/9906074.
[33] S. Mukherjee, B. C. Paul, S. D. Maharaj and A. Beesham, gr-qc/0505103.
[34] A. Beesham, N. A. Hassan and S. D. Maharaj, *Europhys. Lett.* **3** (1987) 1053.
[35] P. Mahato, gr-qc/0603134.
[36] M. Blagojević, *Gravitation and Gauge Symmetries*, Taylor & Francis, 2001
[37] R. T. Hammond, *Rep. Prog. Phys.* **65**, 599 (2002)
[38] F. Gronwald and F. W. Hehl, gr-qc/9602013.
[39] F. W. Hehl, gr-qc/9712096.
[40] V. C. De Andrade, L. C. T. Guillen and J. G. Pereira,

- gr-qc/0011087.
- [41] R. Aldrovandi, J. G. Pereira, K. H. Vu, *Braz. J. Phys.* **34**, 1374 (2004)
- [42] F. W. Hehl, P. von der Heyde, G. D. Kerlick and J. M. Nester, *Rev. Mod. Phys.* **48**, 393 (1976)
- [43] J. M. Nester, *Phys. Rev.* **D16**, 2396 (1977)
- [44] T. Watanabe and M. J. Hayashi, gr-qc/0409029
- [45] S. Capozziello, G. Lambiase and C. Stornaiolo, *Annalen Phys.* **10**, 713 (2001)
- [46] M. Gasperini, *Phys. Rev. Lett.* **56**, 2873 (1986).
- [47] I. L. Shapiro, *Phys. Rept.* **357**, 113 (2002)
- [48] P. Baekler and F. W. Hehl, gr-qc/0601063.
- [49] A. Poltorak, gr-qc/0407060.
- [50] E. W. Mielke, *Phys. Rev. D* **69**, 128501 (2004).
- [51] A. Kleyn, gr-qc/0405028.
- [52] D. Vassiliev, *Annalen Phys.* **14**, 231 (2005)
- [53] A. V. Minkevich and Y. G. Vasilevski, gr-qc/0301098.
- [54] Y. N. Obukhov and J. G. Pereira, *Phys. Rev.* **D67**, 044016 (2003)
- [55] R. Tresguerres, *Phys. Lett. A* **200**, 405 (1995).
- [56] A. D. King and D. Vassiliev, *Class. Quant. Grav.* **18**, 2317 (2001)
- [57] F. Gronwald, *Int. J. Mod. Phys. D* **6**, 263 (1997)
- [58] F. W. Hehl and A. Macias, *Int. J. Mod. Phys. D* **8**, 399 (1999)
- [59] E. A. Poberii, *Gen. Rel. Grav.* **26**, 1011 (1994).
- [60] C. Gruver, R. Hammond and P. F. Kelly, *Mod. Phys. Lett. A* **16**, 113 (2001)
- [61] J. P. Berthias and B. Shahid-Saless, *Class. Quant. Grav.* **10**, 1039 (1993)
- [62] Y. Y. Lam, gr-qc/0211009.
- [63] A. Saa, gr-qc/9309027.
- [64] F. W. Hehl, J. D. McCrea, E. W. Mielke and Y. Neeman, *Phys. Rept.* **258**, 1 (1995)
- [65] E. A. Lord, *Phys. Lett. A* **65**, 1 (1978).
- [66] F. W. Hehl, G. D. Kerlick and P. Von Der Heyde, *Phys. Lett. B* **63**, 446 (1976).
- [67] A. Rajaraman, astro-ph/0311160.
- [68] D. N. Vollick, *Class. Quant. Grav.* **21**, 3813 (2004)
- [69] T. Chiba, *Phys. Lett. B* **575**, 1 (2003)
- [70] I. Antoniadis and S. D. Odintsov, *Mod. Phys. Lett. A* **8**, 979 (1993)
- [71] A. A. Bytsenko, E. Elizalde and S. D. Odintsov, *Prog. Theor. Phys.* **90** 677 (1993)
- [72] L. Fabbri, gr-qc/0608090.
- [73] S. M. Carroll and G. B. Field, *Phys. Rev. D* **50**, 3867 (1994)
- [74] R. Weitzenböck, *Invariantentheorie* (Groningen, P. Noordhoff, 1923); Chap. XIII, Sec.7
- [75] K. Hayashi and T. Shirafuji, *Phys. Rev.* **D19**, 3524 (1979)
- [76] L. I. Schiff, *Phys. Rev. Lett.*, **4**, 215 (1960); *Proc. Nat. Acad. Sci. USA*, **46**, 871 (1960)
- [77] C. M. Will, *Phys. Rev. D* **67**, 062003 (2003)
- [78] R. J. Adler and A. S. Silbergleit, *Int. J. Theor. Phys.* **39**, 1291 (2000)
- [79] J. Biemond, physics/0411129 (2004)
- [80] N. Ashby and B. Shahid-Saless, *Phys. Rev.* **D42**, 1118 (1990)
- [81] B. M. Barker and R. F. O'Connell, *Phys. Rev. D* **2**, 1428 (1970).
- [82] J. W. Moffat, gr-qc/0405091.
- [83] See, *e.g.*, C. W. Misner, K. S. Thorne, J. A. Wheeler, *Gravitation* (W. H. Freeman, 1973); S. Weinberg, *Gravitation and Cosmology : Principles and Applications of the General Theory of Relativity* (Wiley 1972).
- [84] R.P. Kerr, *Phys. Rev. Lett* **11**, 237 (1963)
- [85] R. H. Boyer, R. W. Lindquist, *J. Math. Phys.* **8**, 265 (1967)
- [86] W. de Sitter, M. N. Roy. *Astron. Soc.* **76**, 699 (1916)
- [87] J. Lense and H. Thirring, *Phys. Zeits.* **19**, 156 (1918)
- [88] A. Einstein, (a) *Sitzungsber. Preuss. Akad. Wiss.* 217 (1928); (b) 224 (1928); (c) 2 (1929); (d) 156 (1929); (e) 18 (1930); (f) 401 (1930).
- [89] A. Einstein, W. Mayer, *Sitzungsber. Preuss. Akad. Wiss.*, 110 (1930)
- [90] C. Møller, *K. Dan. Vidensk. Selsk. Mat. Fys. Skr.*, **1**, No.10 (1961).
- [91] C. Pellegrini, J. Plebanski, *K. Dan. Vidensk. Selsk. Mat. Fys. Skr.*, **2**, No.4 (1962).
- [92] C. Møller, *K. Dan. Vidensk. Selsk. Mat. Fys. Skr.*, **89**, No.13 (1978).
- [93] A. Unzicker and T. Case, physics/0503046.
- [94] Y. N. Obukhov and J. G. Pereira, *Phys. Rev. D* **69**, 128502 (2004)
- [95] J. G. Vargas, *Found. Phys.* **22**, 507 (1992).
- [96] J. G. Vargas, D. G. Torr and A. Lecompte, *Found. Phys.* **22**, 527 (1992).
- [97] F. Muller-Hoissen and J. Nitsch, *Phys. Rev. D* **28**, 718 (1983).
- [98] E. W. Mielke, *Annals Phys.* **219**, 78 (1992).
- [99] E. Kreisel, *Annalen Phys.* **36**, 25 (1979).
- [100] H. J. Treder, *Annalen Phys.* **35**, 377 (1978).
- [101] E. Kreisel, *Annalen Phys.* **37**, 301 (1980).
- [102] B. M. Pimentel, P. J. Pompeia and J. F. da Rocha-Neto, *Nuovo Cim.* **120B**, 981 (2005)
- [103] J. W. Maluf and A. Goya, *Class. Quant. Grav.* **18**, 5143 (2001)
- [104] H. I. Arcos and J. G. Pereira, *Class. Quant. Grav.* **21**, 5193 (2004)
- [105] H. I. Arcos and J. G. Pereira, *Int. J. Mod. Phys. D* **13**, 2193 (2004)
- [106] W. R. Stoeger, P. B. Yasskin, *Gen. Rel. Grav.*, **11**, 427 (1979)
- [107] P. B. Yasskin, W. R. Stoeger, *Phy. Rev.* **D21**, 2081 (1980)
- [108] K. Nomura, T. Shirafuji and K. Hayashi, *Prog. Theor. Phys.*, **86**, 1239 (1991)
- [109] H. Kleinert and A. Pelster, *Gen. Rel. Grav.* **31**, 1439 (1999)
- [110] H. Kleinert and A. Pelster, *Acta Phys. Polon. B* **29**, 1015 (1998)
- [111] P. D. D'Eath, *Phys. Rev.* **D11**, 1387 (1975)
- [112] P. D. D'Eath, *Phys. Rev.* **D12**, 2183 (1975)
- [113] S. Hojman, *Phys. Rev.* **D18**, 2741 (1978)
- [114] S. Hojman, M. Rosenbaum and M. P. Ryan, *Phys. Rev.* **D19**, 430 (1979)
- [115] G. Cognola, R. Soldati, L. Vanzo, S. Zerbini, *Phys. Rev.* **D25**, 3109 (1982)
- [116] W. Kopczynski, *Phys. Rev.* **D34**, 352 (1986)
- [117] H. I. Arcos, V. C. de Andrade and J. G. Pereira, *Int. J. Mod. Phys.* **D13**, 807 (2004)
- [118] H. P. Robertson, *Ann. of Math.*, **33**, 496 (1932)
- [119] K. Hayashi and A. Bregman, *Ann. Phys.*, **75**, 562 (1973)
- [120] A. Papapetrou, *Proc. Roy. Soc.* **A209**, 248 (1951)
- [121] W. Adamowicz, A. Trautman, *Bull. Acad. Polon. Sci., Ser. Sci. Math. Astr. Phys.* **23**, 339 (1975)
- [122] B. Bertotti, L. Iess and P. Tortora, *Nature* **425** 374

- (2003).
- [123] S. S. Shapiro, J. L. Davis, D. E. Lebach and J. S. Gregory, Phys. Rev. Lett., **92**, 121101 (2004)
- [124] R. F. C. Vessot *et al.*, Phys. Rev. Lett., **45**, 2081 (1980)
- [125] R. Lakes, Phys. Rev. Lett. **80**, 1826 (1998).
- [126] E. E. Flanagan and E. Rosenthal, arXiv:0704.1447 [gr-qc].
- [127] K. S. Stelle and P. C. West, Phys. Rev. D **21**, 1466 (1980).
- [128] H. R. Pagels, Phys. Rev. D **29**, 1690 (1984).